

# TECHNICAL NOTE

## D-326

LARGE-SCALE WIND-TUNNEL TESTS OF A WINGLESS VERTICAL  
TAKE-OFF AND LANDING AIRCRAFT -  
PRELIMINARY RESULTS

By David G. Koenig and James A. Brady

Ames Research Center  
Moffett Field, Calif.

NATIONAL AERONAUTICS AND SPACE ADMINISTRATION  
WASHINGTON

October 1960



## NATIONAL AERONAUTICS AND SPACE ADMINISTRATION

## TECHNICAL NOTE D-326

## LARGE-SCALE WIND-TUNNEL TESTS OF A WINGLESS VERTICAL

## TAKE-OFF AND LANDING AIRCRAFT -

## PRELIMINARY RESULTS

By David G. Koenig and James A. Brady

## SUMMARY

Large-scale wind-tunnel tests were made of a wingless vertical take-off and landing aircraft at zero sideslip to determine performance and longitudinal stability and control characteristics at airspeeds from 0 to 70 knots. Roll control and rudder effectiveness were also obtained. Limitations in the propulsion system restricted the lift for which level flight could be simulated to approximately 1500 pounds.

Test variables with roll control and rudder undeflected were airspeed, vane setting, angle of attack, elevator deflection, and power. In most of the tests angle of attack, elevator, and power were varied individually while the other four parameters were held constant at previously determined values required for simulating trimmed level flight. The majority of the tests were made with power on and tail on at airspeeds between 20 and 70 knots. However, a limited number of data were obtained for the following conditions: (1) at zero velocity, horizontal tail on, power on, (2) at forward velocity, tail off and power on, (3) at forward velocity, tail on, but with power off.

## INTRODUCTION

There has been research and development work on several types of aircraft with vertical take-off and landing capabilities. One type is a wingless aircraft configuration. A description of the development and construction of a large-scale test bed of such a configuration is presented in reference 1. The aircraft attains a major portion of its vertical lift in hovering and forward flight by diverting downward most of the air drawn through a duct by counterrotating ducted propellers; downward deflection is obtained by means of a series of duct exit vanes. One set of vanes located at the duct exit is adjustable so that as forward flight speed is increased, the deflection of the duct air flow can be reduced. The other vanes are not adjustable and are placed in such a manner that they deflect the air downward, approximately 30° from the forward duct center line, before it flows through the adjustable vanes.

An elevator and a rudder serve both as conventional control surfaces at forward speed, and as a means of deflecting the air which is ducted back to the tail from the main duct for longitudinal and directional control in hovering or very low-speed flight.

Large-scale wind-tunnel tests of this test bed have been undertaken in order to explore the performance, stability, and control characteristics during transition from hovering to forward flight. Tests were limited to an airspeed range of from 0 to 70 knots by both a lower limit in duct air-flow deflection angle (with respect to the main duct center line) of approximately  $30^\circ$  and limits in the power absorption characteristics of the fixed-pitch propellers used for the tests.

Results of the tests are presented herein without discussion in order to expedite publication.

A  
4  
2  
0

#### NOTATION

$C_L$	$\frac{\text{lift}}{qS}$	
$C_D$	$\frac{\text{drag}}{qS}$	
$C_l$	$\frac{\text{rolling moment}}{qSd}$	, with reference to axis parallel with free stream
$C_n$	$\frac{\text{yawing moment}}{qSd}$	
$C_Y$	$\frac{\text{side force}}{qS}$	
$C_m$	$\frac{\text{pitching moment}}{qSd}$	
$d$	mean internal duct diameter, ft	
$P$	total engine chart power, hp	
$q$	free-stream dynamic pressure, averaged for a particular control or power sweep, lb/sq ft	
$S$	reference area, $\left(\frac{\pi}{4}\right) d^2$ , sq ft	
$V_\infty$	nominal airspeed, k	
$\alpha$	angle of attack of the aircraft reference plane (see fig. 2(b)) with respect to wind-tunnel walls, deg	

- $\delta_a$  roll control deflection, deg
- $\delta_e$  elevator deflection, deg
- $\delta_r$  rudder deflection, deg
- $\theta$  angle between the lower surface of the cascaded vanes and the aircraft reference plane, deg (see fig. 2(d))
- $\theta_F$  angle between the lower surface of the single forward vane and the aircraft reference plane, deg (see fig. 2(d))

#### AIRCRAFT AND TEST EQUIPMENT

A photograph of the test bed mounted in the 40- by 80-Foot Wind Tunnel is presented in figure 1. A three-quarter rear view of the aircraft is shown in figure 2(a), and a sketch with pertinent dimensions is shown in figure 2(b). Other geometrical data are listed in table I. Contours of the inner and outer surfaces are shown in figure 2(c). Details of the turning vane system and roll control are presented in figure 2(d). Pertinent details of the tail are presented in figure 2(e), and coordinates of the airfoil section of the tail are presented in table II. Blade angles, chord, and thickness ratio of the propeller are shown in figure 2(f).

The internal flow system of the test bed may be described in the following manner. Ninety percent of the total mass flow passes through the system of vanes to provide lift; the remaining 10 percent of the mass flow is directed over the mid 27-percent span of the elevator and the lower 28 percent of the rudder. The turning vanes are a system of both fixed (vanes B, C, and F in fig. 2(d)) and adjustable vanes. The adjustable vanes consist of a set of 5 mechanically linked cascade vanes (vanes D and E in fig. 2(d)) of deflection  $\theta$ , as well as a single adjustable vane (vane A, fig. 2(d)) with deflection,  $\theta_F$ . The single adjustable vane was set at  $\theta_F = 66^\circ$  for airspeeds up to 40 knots and  $31^\circ$  for airspeeds between 40 and 70 knots. The cascade vane deflections were limited to values of  $\theta$  between  $33^\circ$  and  $70^\circ$ . The single upper fixed vane (vane F) shown in figure 2(d) was used only for part of the testing done at 0, 20, and 30 knots. Roll control was obtained by deflecting the hinged surface located on the ventral fin.

The two fixed-pitch propellers rotated in opposite directions and each one was driven by a 265 horsepower reciprocating engine. The propeller was designed (see fig. 2(f)) so that only part of the total engine power available could be absorbed during the tests without exceeding the maximum engine speed specified for the engines.

The aircraft was mounted on a metal frame which was, in turn, mounted on the conventional strut system. Strain-gage load cells were placed between the frame and the struts at the three attachment points to measure the longitudinal aerodynamic forces.

## TESTS AND PROCEDURE

The procedure for testing with power and horizontal tail on and with rudder and roll control undeflected was as follows for most of the vane setting and airspeed combinations considered. Values of angle of attack, elevator deflection, and power settings required to trim the aircraft at 1500 pounds lift and zero drag were determined approximately by trial and error. Data were then obtained while these three parameters were varied individually with the other two held constant at approximately their initial values.

A  
4  
2  
0

In addition to the aforementioned tests, a limited number of tests with roll control and rudder undeflected, for which results are presented herein, were made under the following conditions:

1. With zero velocity at  $20^\circ$  angle of attack and varying power or elevator deflection.
2. With forward velocity, power on, but horizontal tail off.
3. With forward velocity, power off, horizontal tail on.

Tests with either varying roll control deflection or rudder deflection were made at one combination of  $\theta$  and  $\theta_F$  per airspeed for airspeeds from 20 to 70 knots. Values of angle of attack, elevator setting, and power were those required to simulate approximately trimmed level flight (1500 lb lift).

The value of 1500 pounds used as trimmed lift was arbitrarily chosen as the maximum which could be obtained for the complete test airspeed range and was controlled essentially by the capacity of the propulsion system.

## DATA REDUCTION

The values of  $C_L$ ,  $C_D$ , and  $C_m$  presented herein were computed from the outputs of strain-gaged load cells located at the three attachment points between the aircraft and the steel frame.

The values of  $C_Y$ ,  $C_n$ , and  $C_l$  were derived from wind-tunnel mechanical scale system readings, and include forces exerted on the support strut tips and supporting frame as well as on the aircraft.

No corrections for wind-tunnel-wall effects or possible influences of the support frame on the measured aerodynamic characteristics have been considered.

### Least Count Errors

The following are the estimated errors of measurement of both the test variables and measured values of forces and moments as based on the least count of the respective read-out systems:

$\alpha$	$\pm 0.2^\circ$	Yawing moment	$\pm 70$ ft-lb
Lift	$\pm 10$ lb	Rolling moment	$\pm 160$ ft-lb
Drag	$\pm 10$ lb	$q$	$\pm 0.02$ lb/sq ft
Pitching moment	$\pm 80$ ft-lb	$\delta_e, \delta_a, \delta_r,$ and $\theta$	$\pm 1/4^\circ$
Side force	$\pm 4$ lb	$P$	$\pm 5$ hp

### Power Measurement

Values of power listed herein were obtained from the manufacturer's engine performance charts. Since the engines in the test bed had been used considerably prior to the subject installation, the use of chart power may be only an approximation of actual engine output. However, the method of measuring power was found sufficiently reliable to enable the repetition of test conditions satisfactorily.

### Scatter in Data

Extreme flexibility in the test-bed structure seemed to be the principal source of scatter in the data for a given set of test conditions. The situation seemed to be augmented for the tests at 0 and 20 knots by the random flow recirculation within the wind-tunnel test section.

## RESULTS

### Presentation of Force and Moment Data

Values of  $C_L$ ,  $C_D$ , and  $C_m$  for the aircraft with various combinations of vane configuration and airspeed as obtained with angle of attack varying are presented in figures 3(a) through (f). It should again be

mentioned that only two settings of vane A (fig. 2(d)),  $\theta_F$ , were considered in the test:  $66^\circ$  for airspeed from 0 to 40 knots, and  $31^\circ$  for airspeed from 40 to 70 knots.

Values of  $C_L$ ,  $C_D$ , and  $C_m$  for the aircraft as functions of power for various combinations of vane settings and airspeed are presented in figures 4(a) through (f). The vane settings and airspeed are similar to those used in obtaining the data of figure 3.

Values of  $C_L$ ,  $C_D$ , and  $C_m$  obtained with the elevator deflection varying at each of the airspeeds considered in the present tests are presented in figures 5(a) and (b). Data for only one vane configuration per airspeed are presented since it was found that elevator effectiveness was almost independent of vane configuration for the combinations of vane configuration and speed considered.

Results of less extensive portions of the testing are presented in the figures listed as follows. Figure 6 shows data obtained while varying angle of attack with the horizontal tail off. Data from variable angle-of-attack tests with power off are presented in figure 7. Force and moment data from tests at zero velocity are presented in figure 8 for the aircraft at  $20^\circ$  angle of attack with both power and elevator deflection as variables. Values of  $C_Y$ ,  $C_n$ , and  $C_l$  are presented in figure 9 for tests in which either roll control or rudder deflection were varying.

A  
4  
2  
0

#### Characteristics in Trimmed Level Flight

For most of the combinations of vane configuration and airspeed for which data have been presented, trimmed level flight for 1500 pounds of lift was only approximately simulated. In order to estimate control and power adjustments from the test values which would be required to more nearly simulate trimmed level flight conditions ( $L = 1500$  lb,  $C_D$  and  $C_m = 0$ ) the following equations were solved:

$$C_{L_\alpha} \Delta\alpha + C_{L_{\delta_e}} \Delta\delta_e + C_{L_P} \Delta P = \Delta J_L$$

$$C_{D_\alpha} \Delta\alpha + C_{D_{\delta_e}} \Delta\delta_e + C_{D_P} \Delta P = \Delta J_D$$

$$C_{m_\alpha} \Delta\alpha + C_{m_{\delta_e}} \Delta\delta_e + C_{m_P} \Delta P = \Delta J_m$$

where  $\Delta\alpha$ ,  $\Delta\delta_e$ , and  $\Delta P$  are the adjustments in  $\alpha$ ,  $\delta_e$ , and  $P$  required to simulate more nearly level flight conditions by changing test values of  $C_L$ ,  $C_D$ , and  $C_m$  by the amounts  $\Delta C_L$ ,  $\Delta C_D$ , and  $\Delta C_m$ ;  $C_{L_\alpha}$ ,  $C_{L_{\delta_e}}$ ,  $C_{L_P}$ ,  $C_{D_\alpha}$ ,  $C_{D_{\delta_e}}$ ,  $C_{D_P}$ ,  $C_{m_\alpha}$ ,  $C_{m_{\delta_e}}$ ,  $C_{m_P}$  . . . are slopes of the experimental curves obtained from the data of figures 3 through 5 for approximately level-flight conditions.



The resulting values of  $\alpha$ ,  $\delta_e$ , and  $P$  are presented in figure 10 as a function of vane angle,  $\theta$ . Two transitions defined as given variations of vane angle with airspeed are described in figure 11. Corresponding variations of angle of attack, elevator deflection, power, and stability,  $dC_m/dC_L$ , are indicated in the figure.

Ames Research Center

National Aeronautics and Space Administration  
Moffett Field, Calif., April 22, 1960

#### REFERENCE


1. Anon.: Final Report on Research on Wingless Aircraft. Collins Aeronautical Research Laboratories, July 1, 1959.

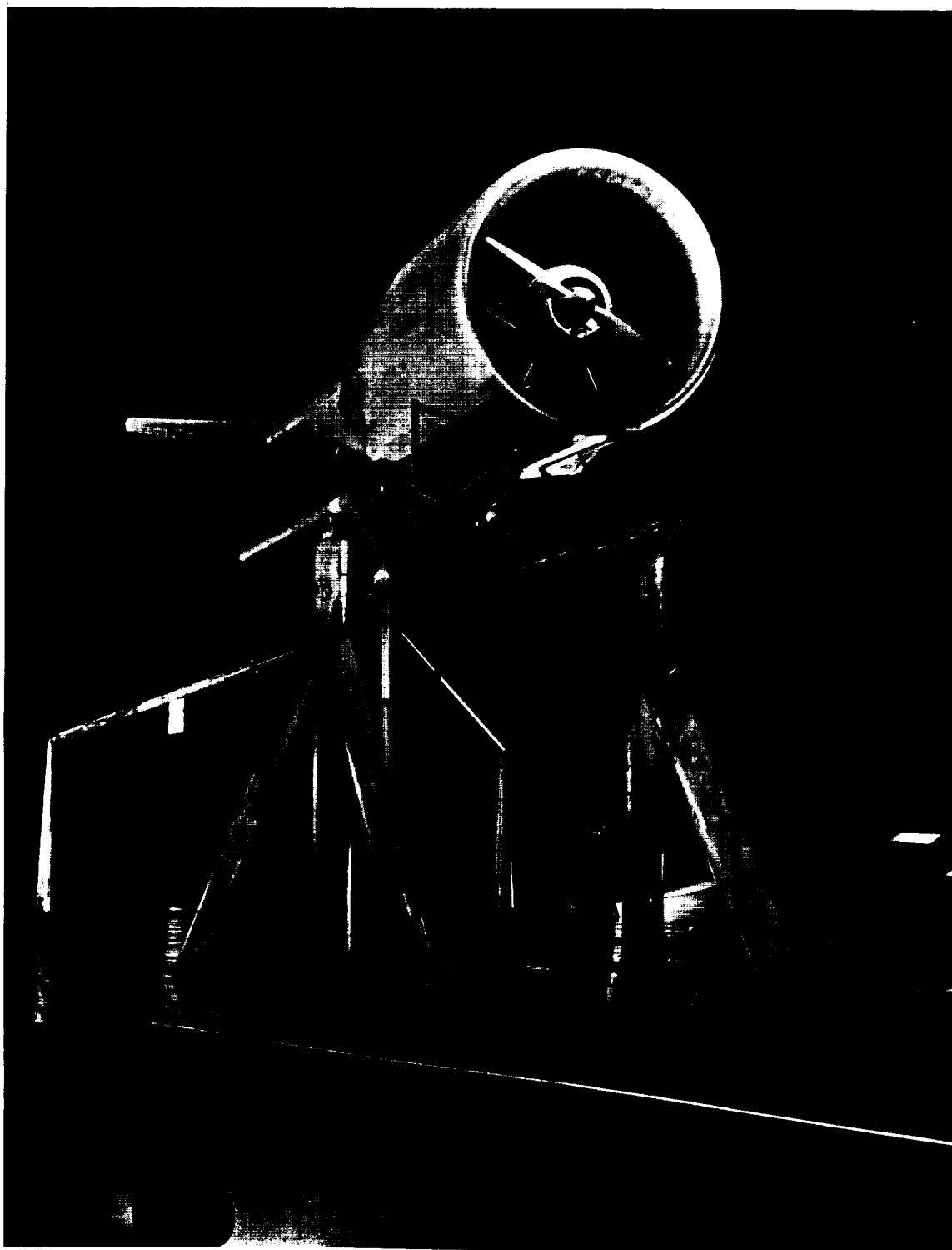
A  
4  
2  
0

TABLE I.- GEOMETRIC DATA

Duct area (including nacelle), sq ft . . . . .	44.18
Duct area (excluding nacelle), sq ft . . . . .	37.12
Diameter, ft . . . . .	7.5
Exhaust area (in plane 30° from horizontal plane), sq ft . . . . .	58
Over-all width, ft . . . . .	9.17
Moment center (location from duct leading edge), ft . . . . .	10.83
Horizontal tail	
Span, ft . . . . .	18.58
Area (extended to plane of symmetry), sq ft . . . . .	100.6
Aspect ratio . . . . .	3.43
Taper ratio . . . . .	0.438
Incidence of lower surface, deg . . . . .	0
Elevator area, sq ft . . . . .	59.5
Elevator hingeline to moment center . . . . .	26.83
Rudder area, sq ft . . . . .	27
Roll-control area, sq ft . . . . .	11.55
Engines, (two) Lycoming O435-17, hp . . . . .	265
Propeller diameter, ft . . . . .	7.35

A  
4  
2  
0TABLE II.- COORDINATES OF AIRFOIL SECTION OF HORIZONTAL TAIL  
[Section is Parallel With Aircraft Plane of Symmetry]

Percent chord		
Station	Ordinates	
	Upper surface	Lower surface
0	3.54	3.54
1.25	5.56	1.93
2.5	6.53	1.37
5.0	7.92	.75
7.5	8.89	.39
10	9.68	.21
15	10.72	.04
20	11.35	0
25	11.73	
30	11.96	
40	11.83	
50	11.04	
60	9.69	
70	7.87	
80	5.54	
90	2.88	
100	.12	
L.E.R., 146; center at station 146 and 3.60 above the lower surface.		

A  
4  
2  
0

A-25698

Figure 1.- Aircraft as mounted in Ames 40- by 80-Foot Wind Tunnel.



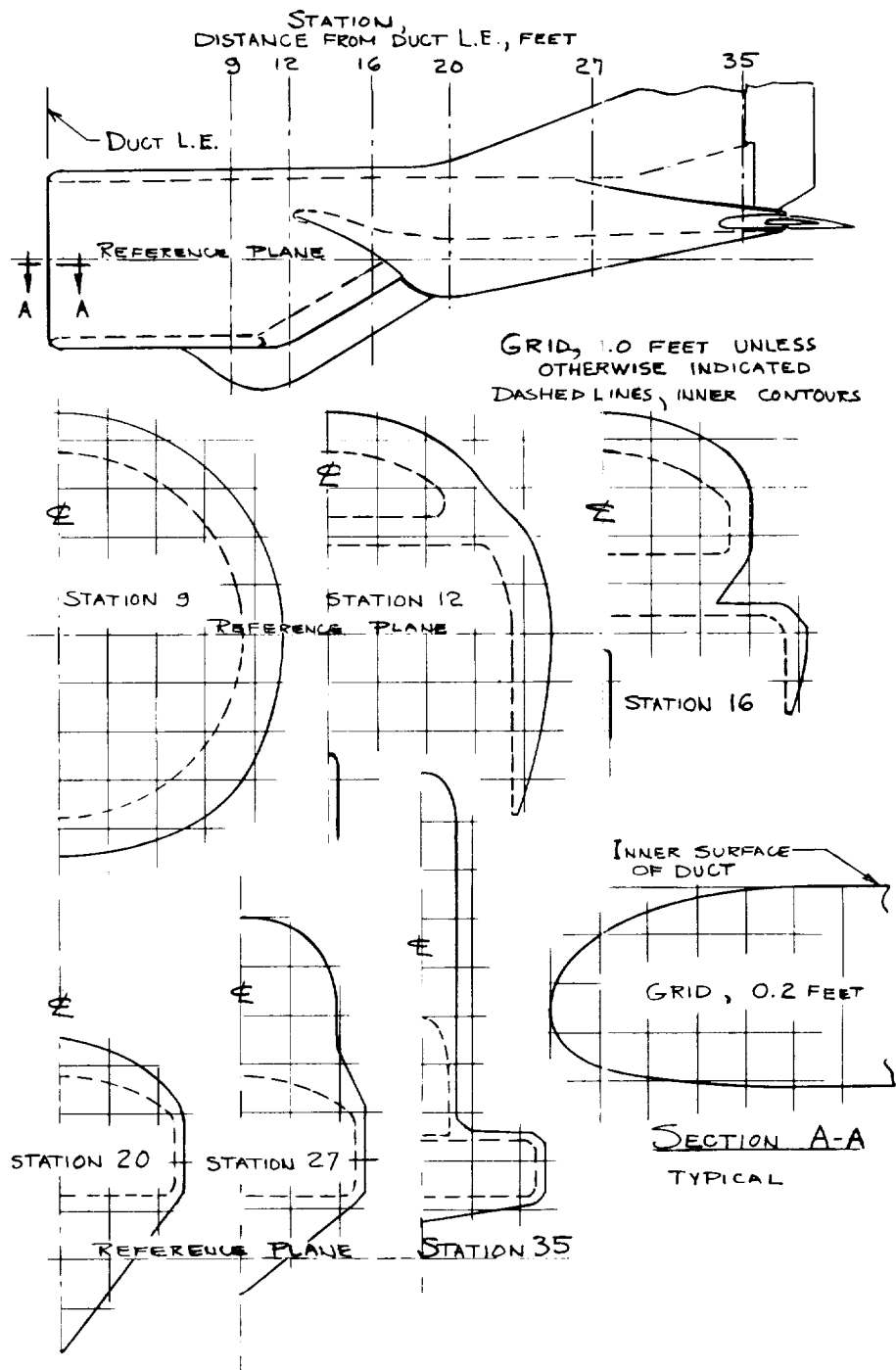
A-25510

(a) Three-quarter rear view of the aircraft.

Figure 2.- Geometric details of the aircraft.

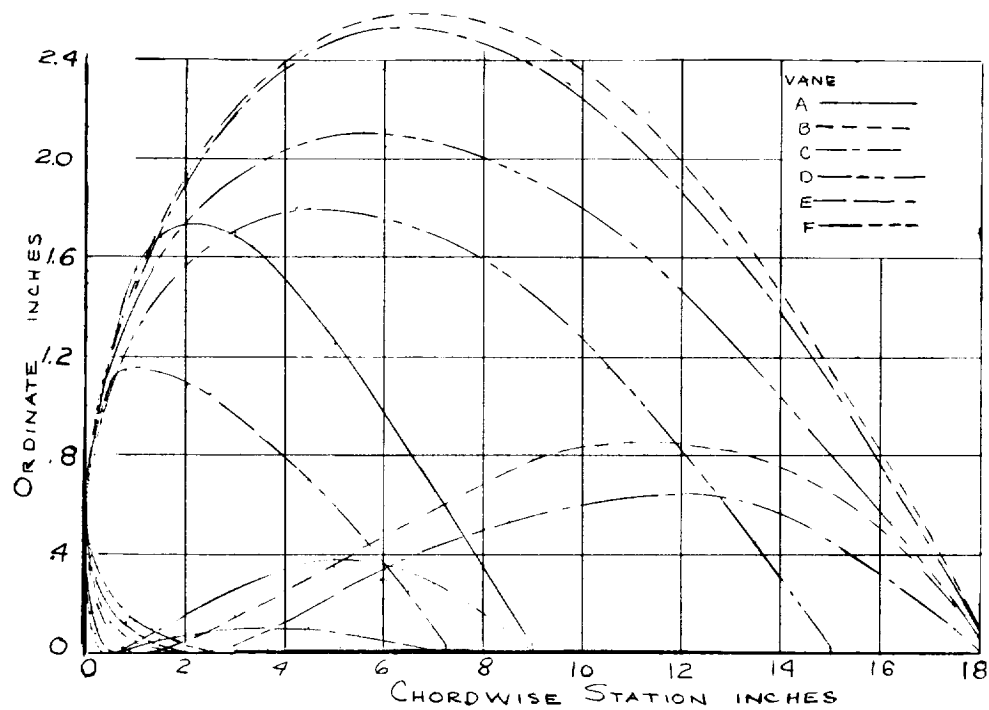
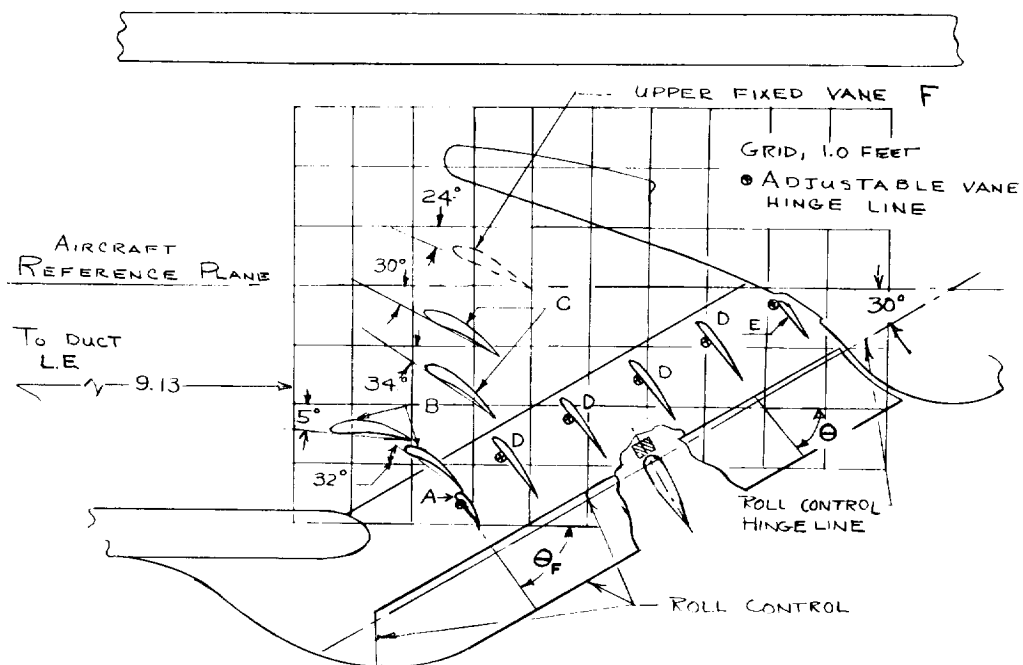
A  
4  
2  
0



A  
4  
2  
0

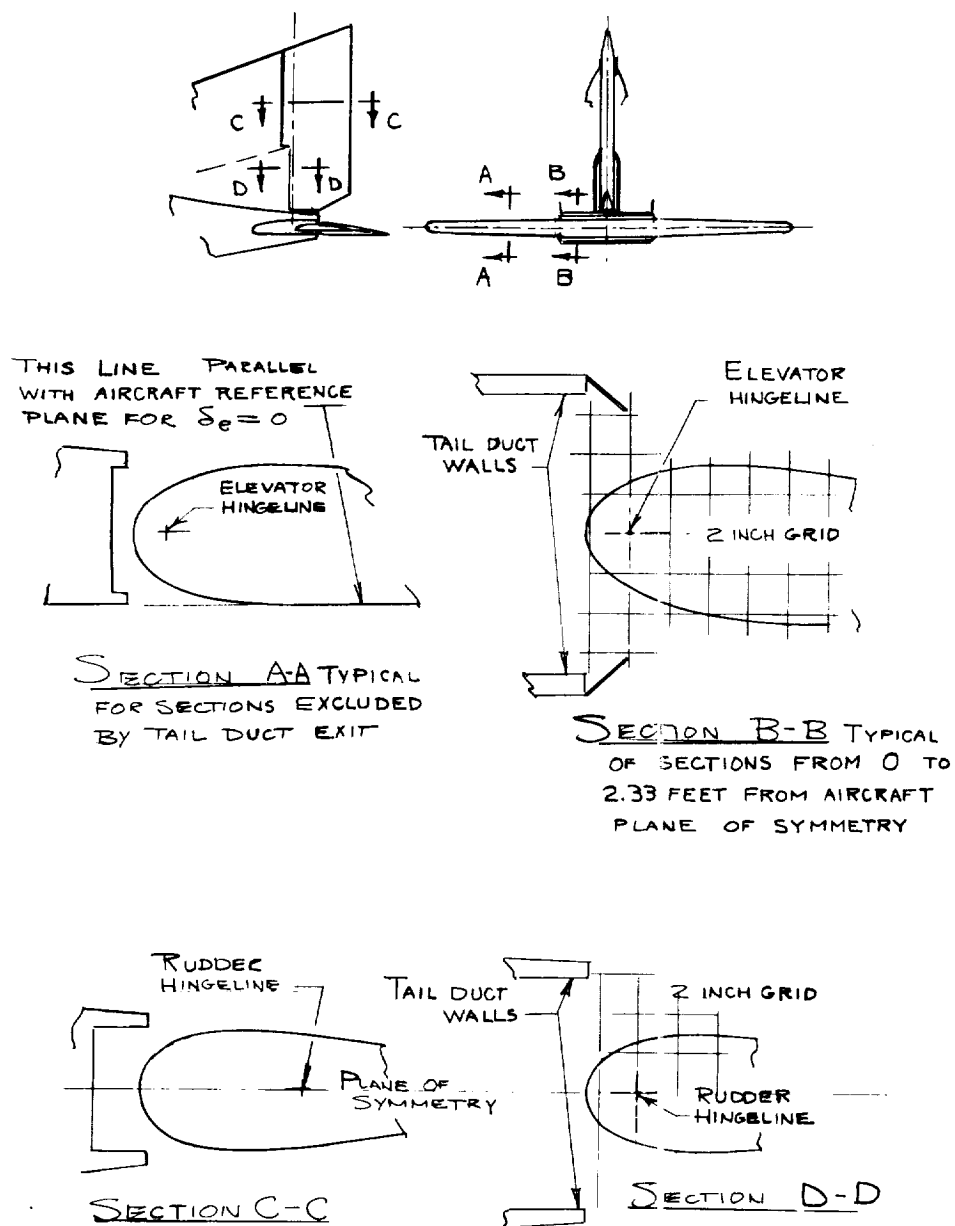
(c) Aircraft contours.

Figure 2.- Continued.



(d) Detail of turning vane system and roll vane.

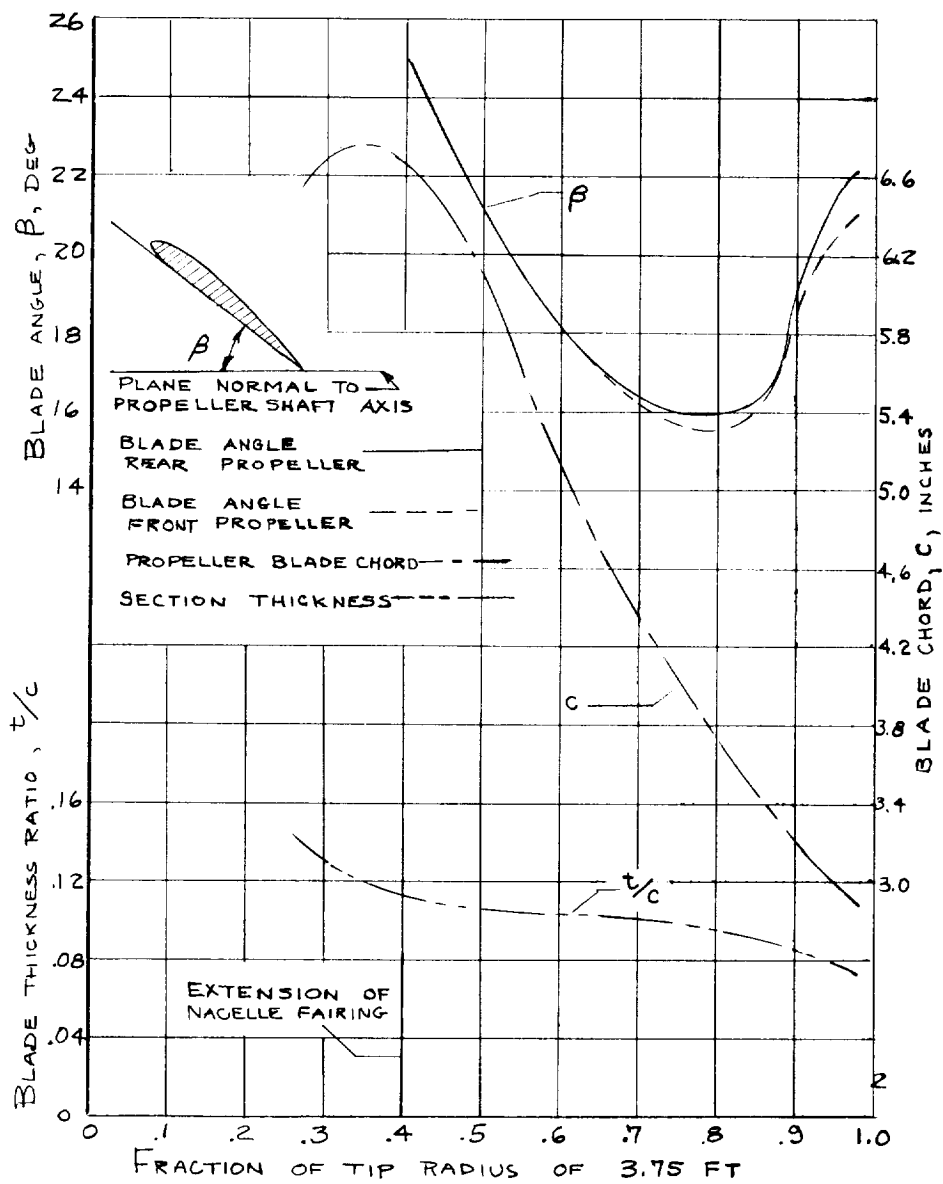
Figure 2.- Continued.



(e) Details of the tail.

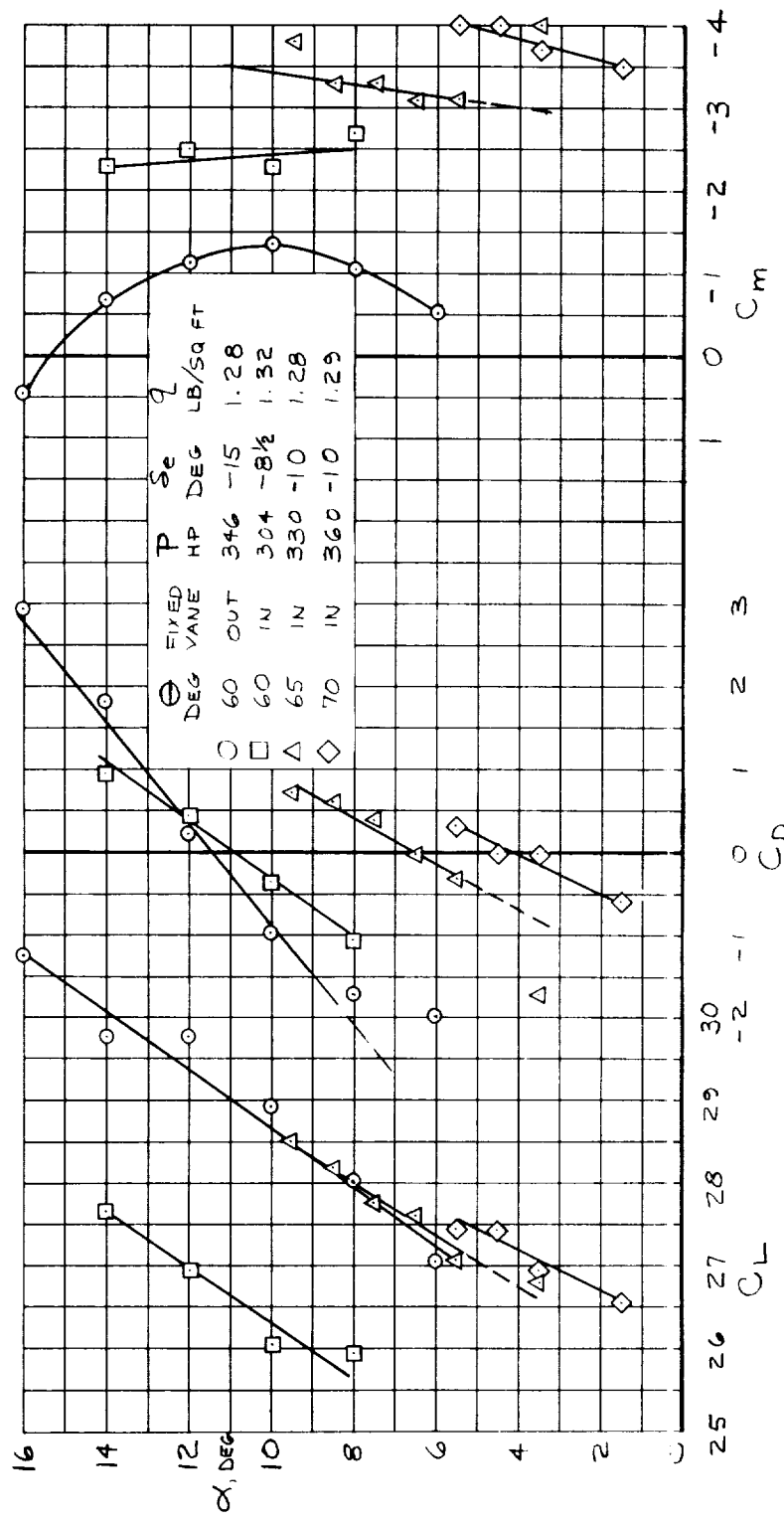
Figure 2.- Continued.





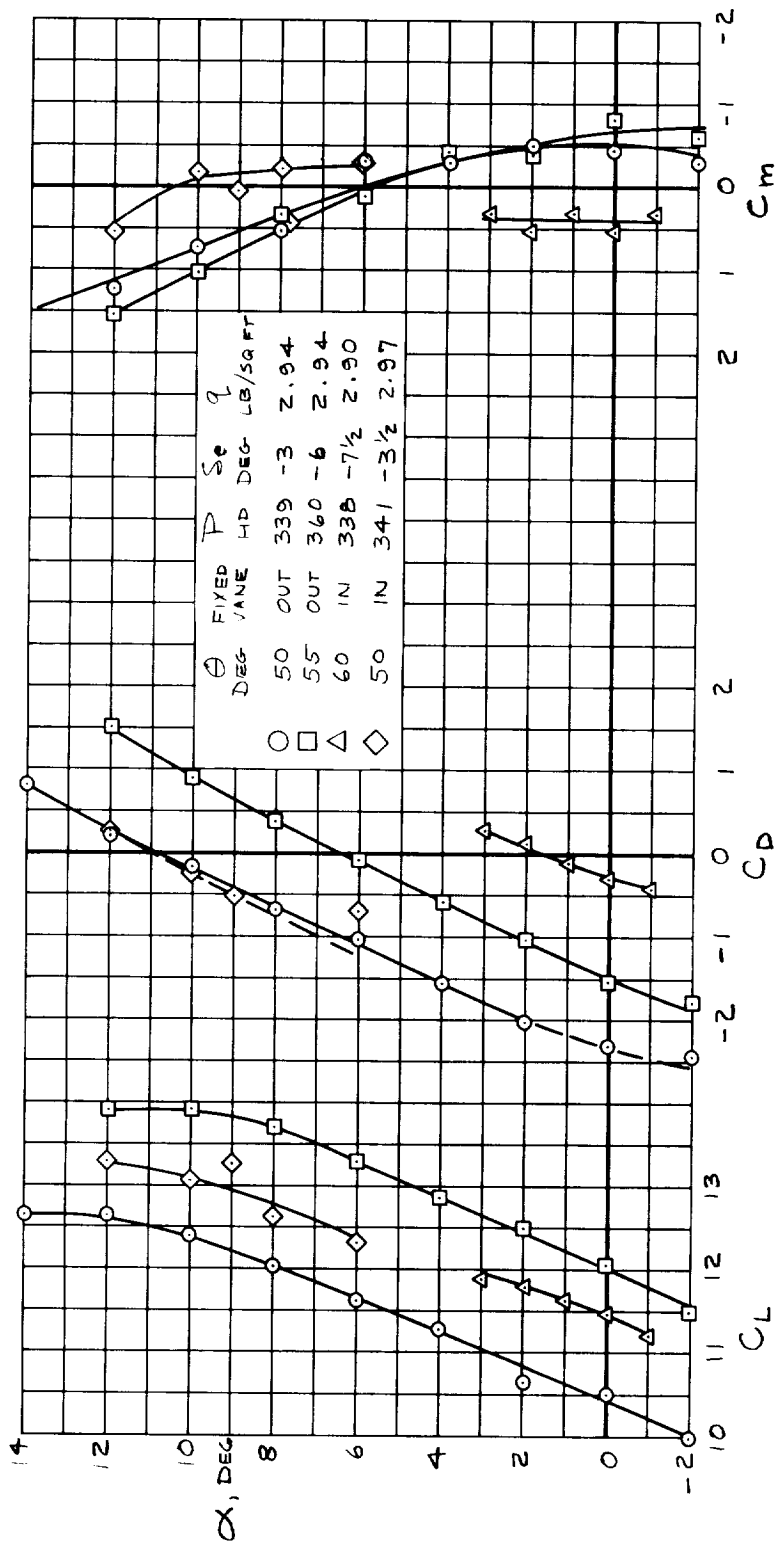
(f) Propeller configuration.

Figure 2.- Concluded.



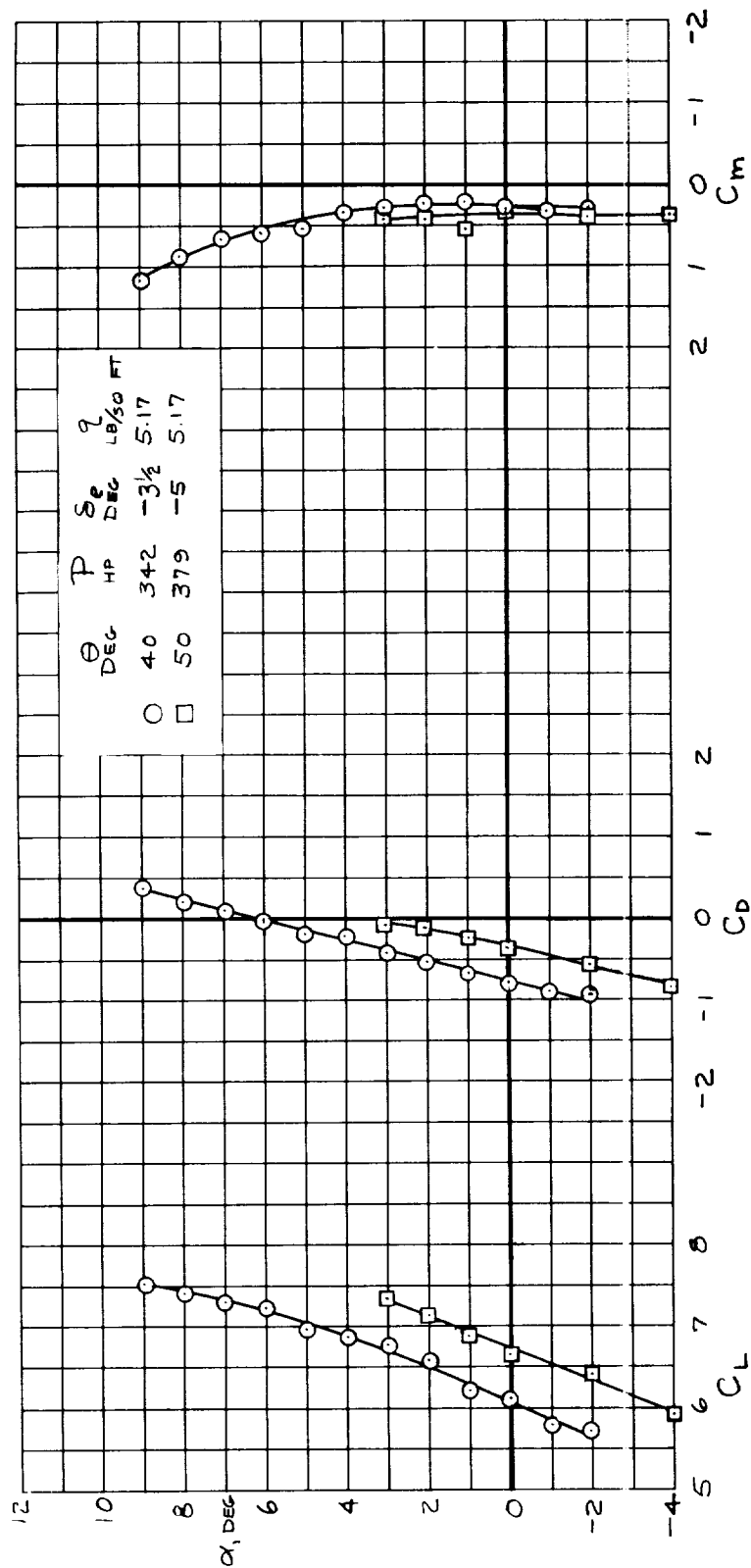
(a)  $V_\infty = 20$  knots;  $\theta_F = 66^\circ$ .

Figure 3.- Characteristics of the aircraft with the horizontal tail on; angle of attack varying; fixed vane, F, out unless noted otherwise.



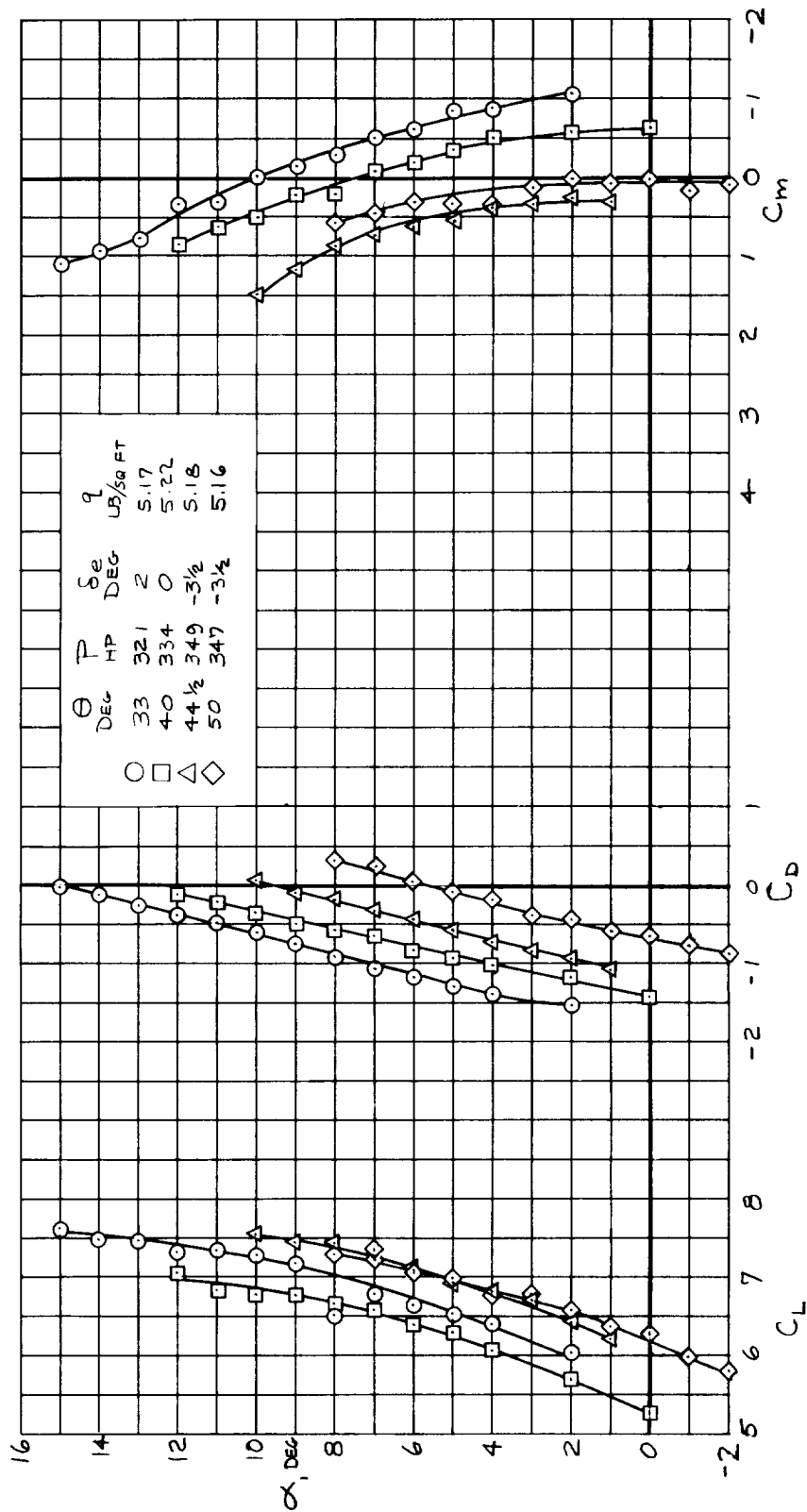
(b)  $V_\infty = 30$  knots;  $\theta_F = 66^\circ$ .

Figure 3.- Continued.



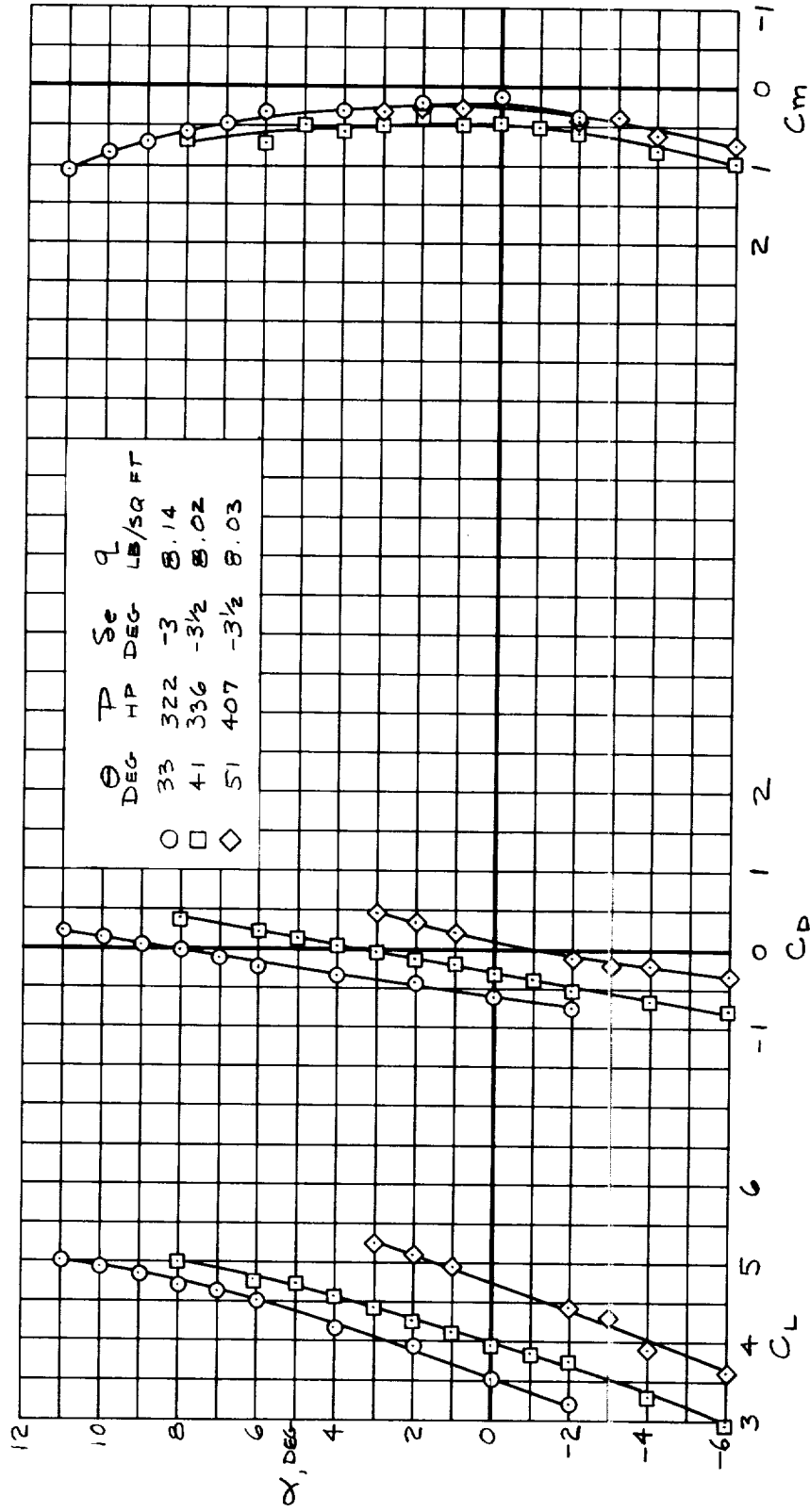
(c)  $V_\infty = 40$  knots;  $\theta_F = 66^\circ$ .

Figure 3.- Continued.



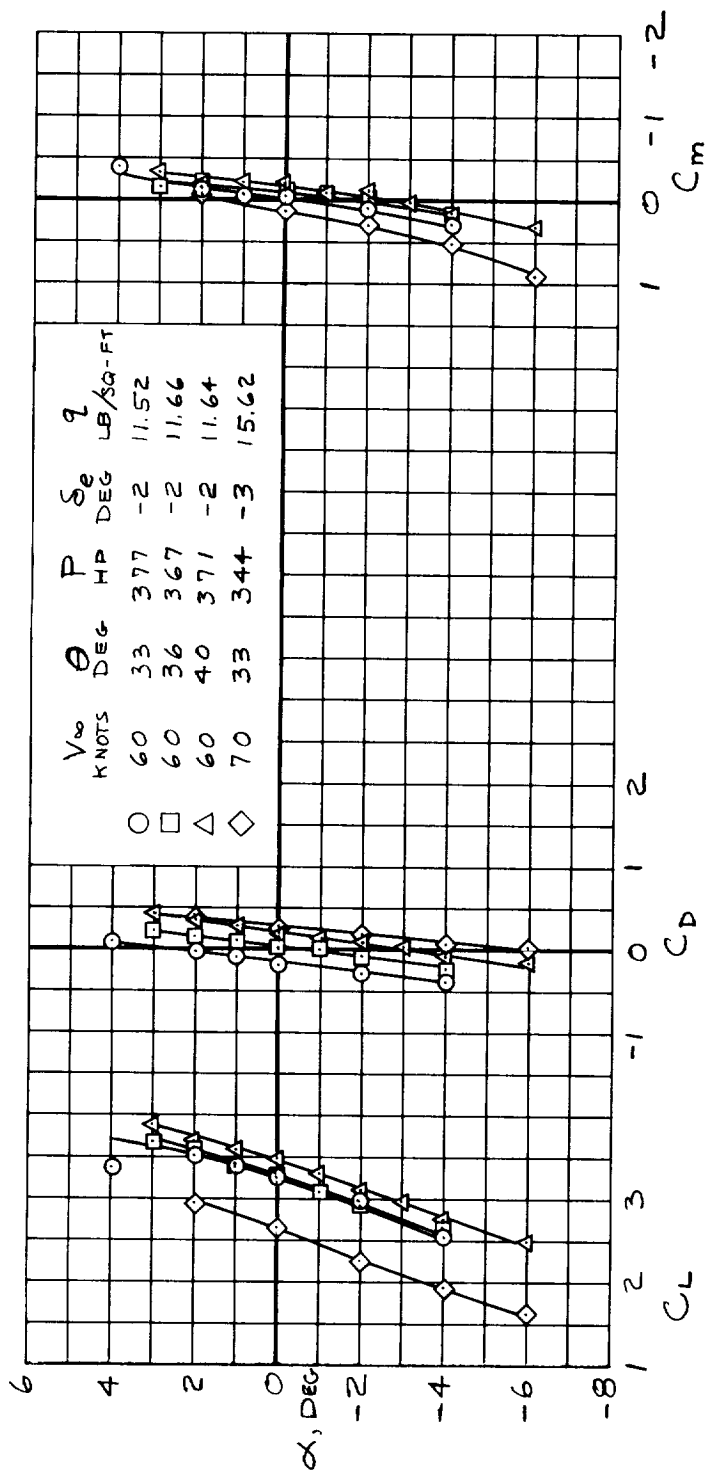
(d)  $V_\infty = 40$  knots;  $\theta_F = 31^\circ$ .

Figure 3.- Continued.



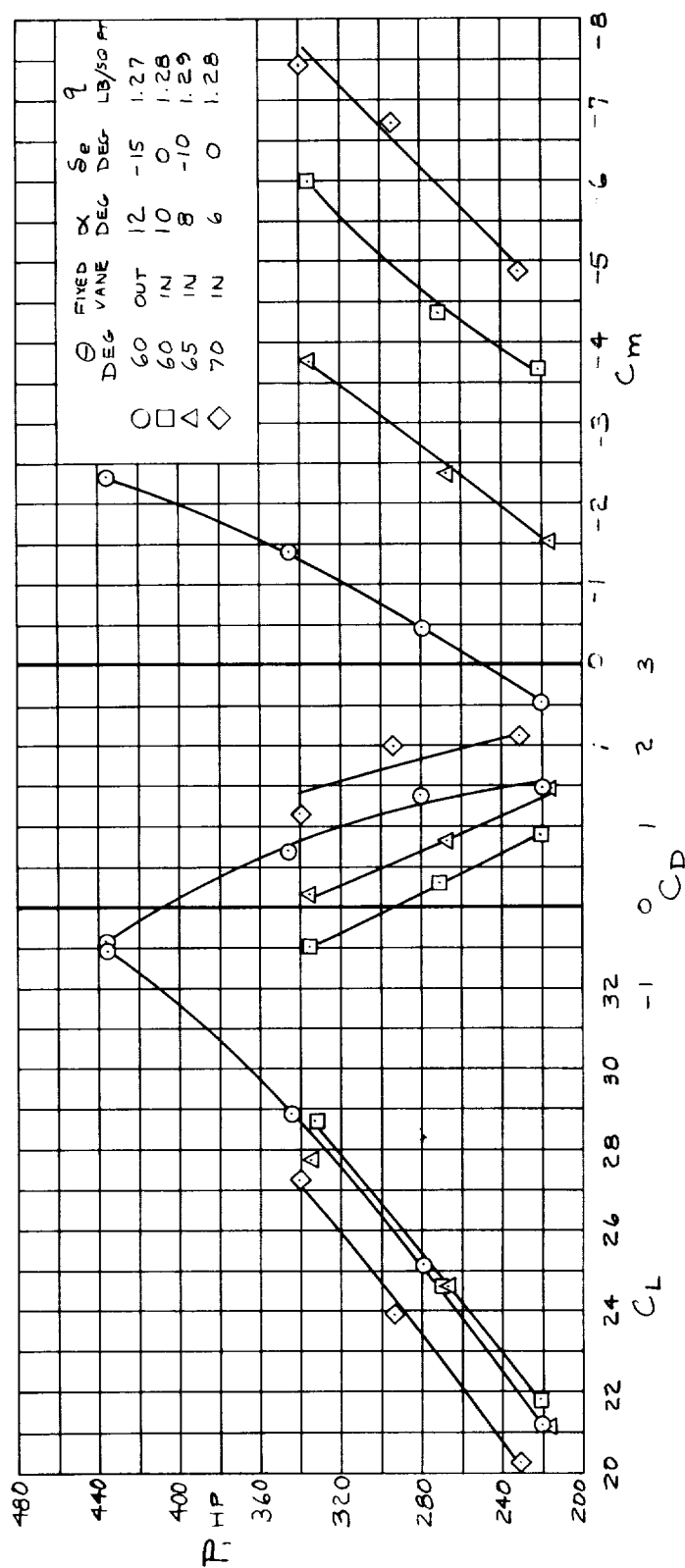
(e)  $V_\infty = 50$  knots;  $\theta_F = 31^\circ$ .

Figure 3.- Continued.



(f)  $V_\infty = 60$  and  $70$  knots;  $\theta_F = 31^\circ$ .

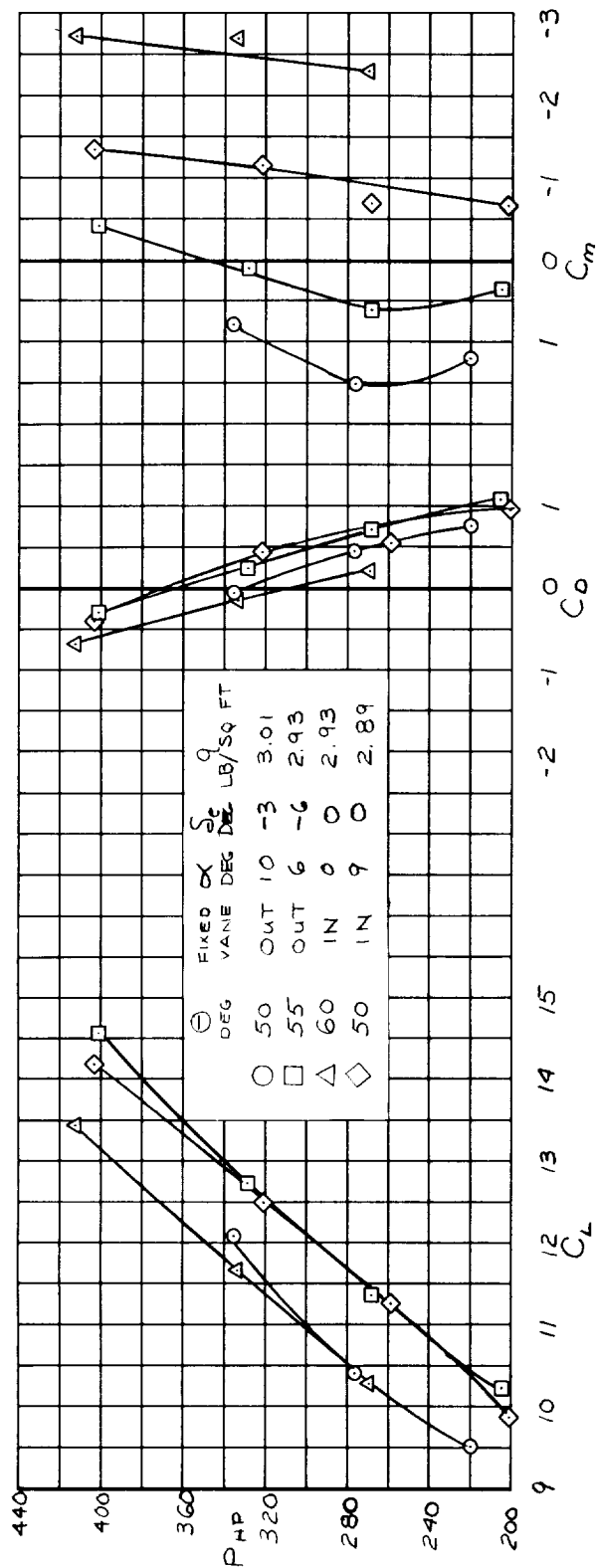
Figure 3.- Concluded.



(a)  $V_\infty = 20$  knots;  $\theta_F = 66^\circ$ .

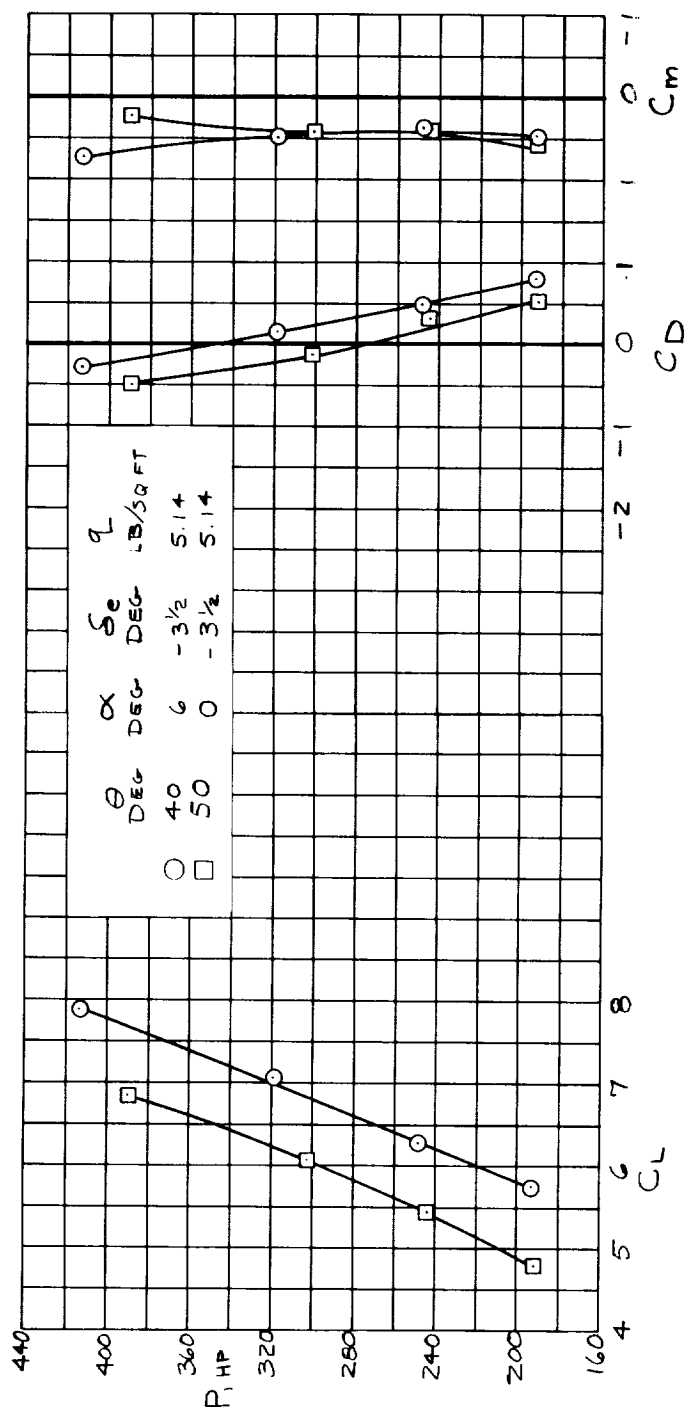
Figure 4.- Characteristics of the aircraft with the horizontal tail on; power varying; fixed vane,  $F$ , out unless noted otherwise.





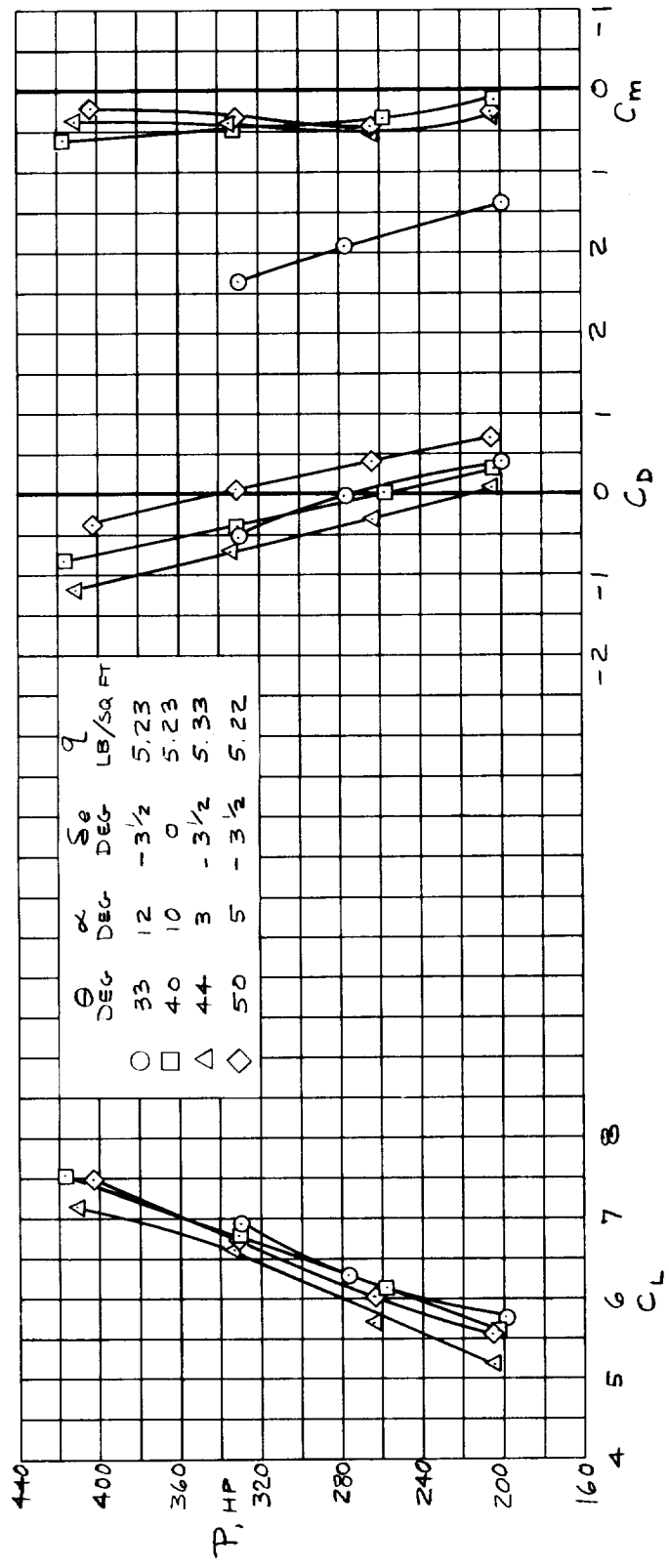
(b)  $V_\infty = 30$  knots;  $\theta_F = 66^\circ$ .

Figure 4.- Continued.



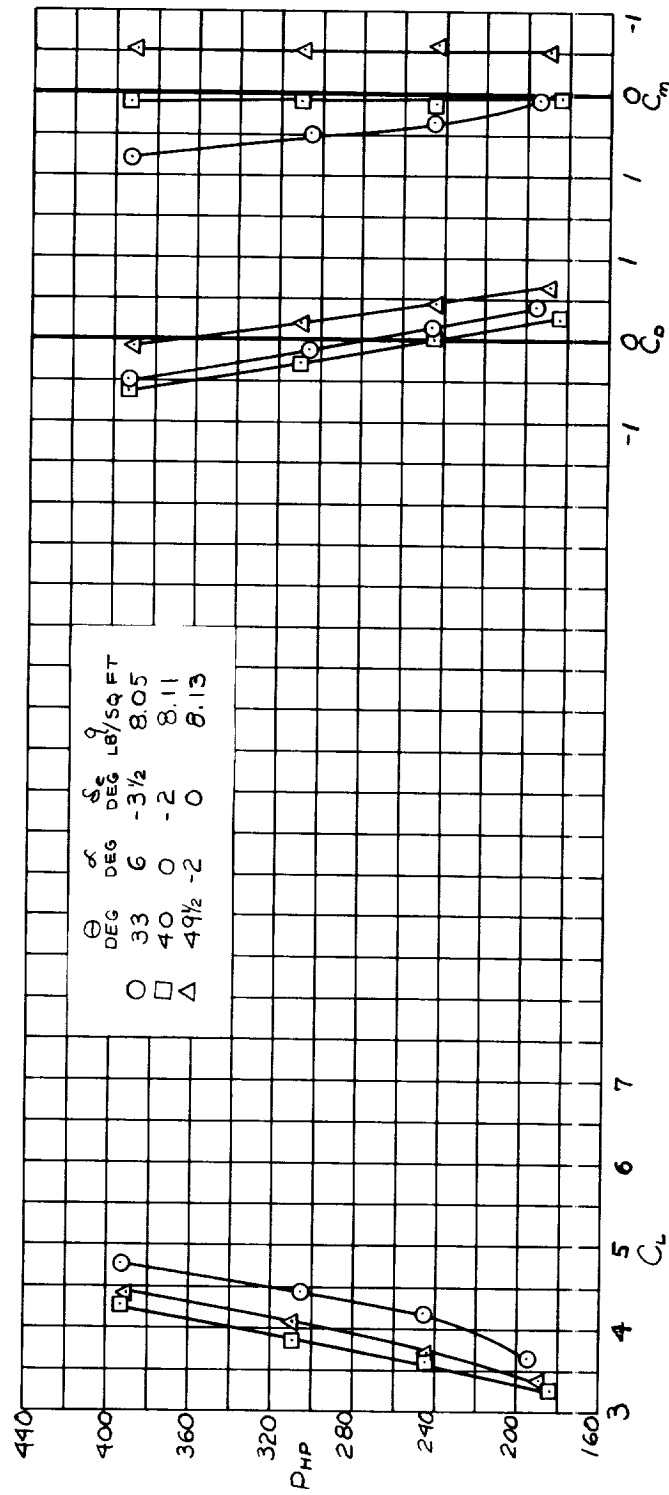
(c)  $V_\infty = 40$  knots;  $\theta_F = 66^\circ$ .

Figure 4.- Continued.



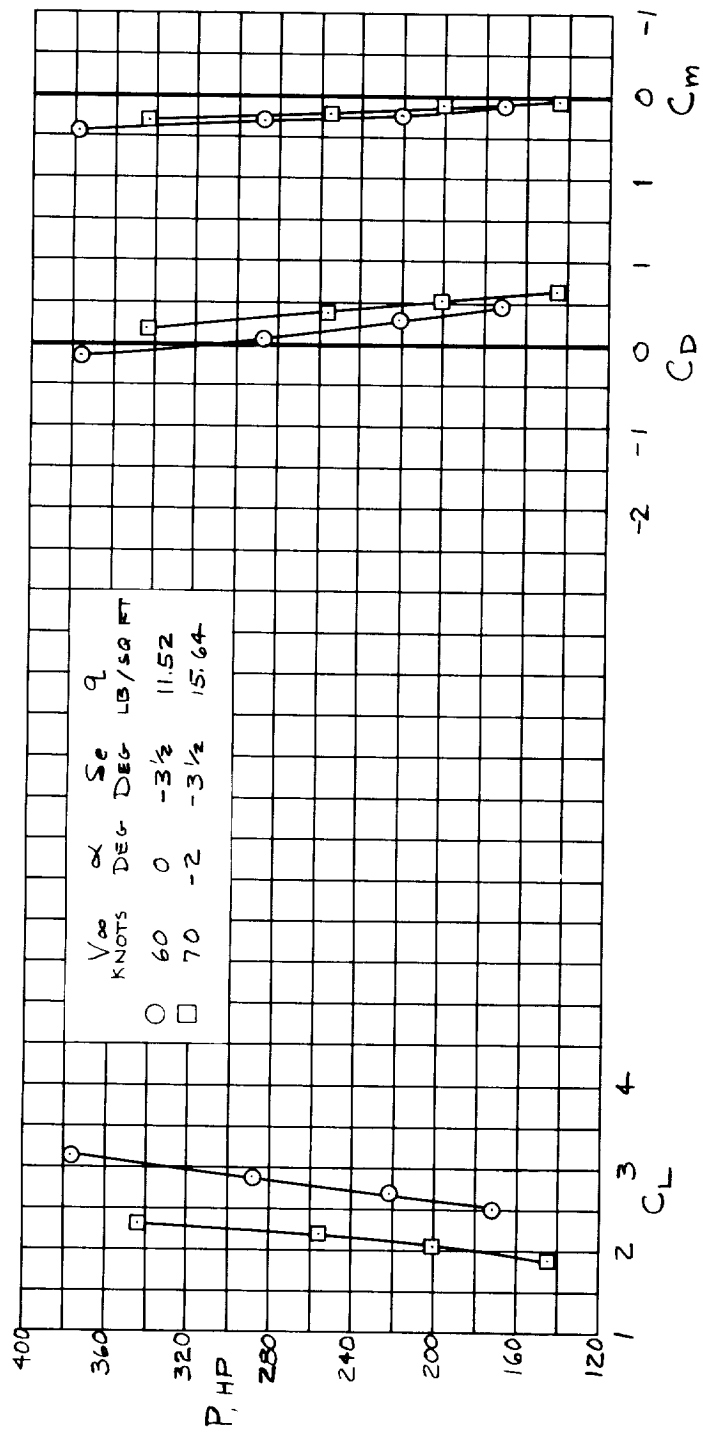
(d)  $V_\infty = 40$  knots;  $\theta_F = 31^\circ$ .

Figure 4.- Continued.



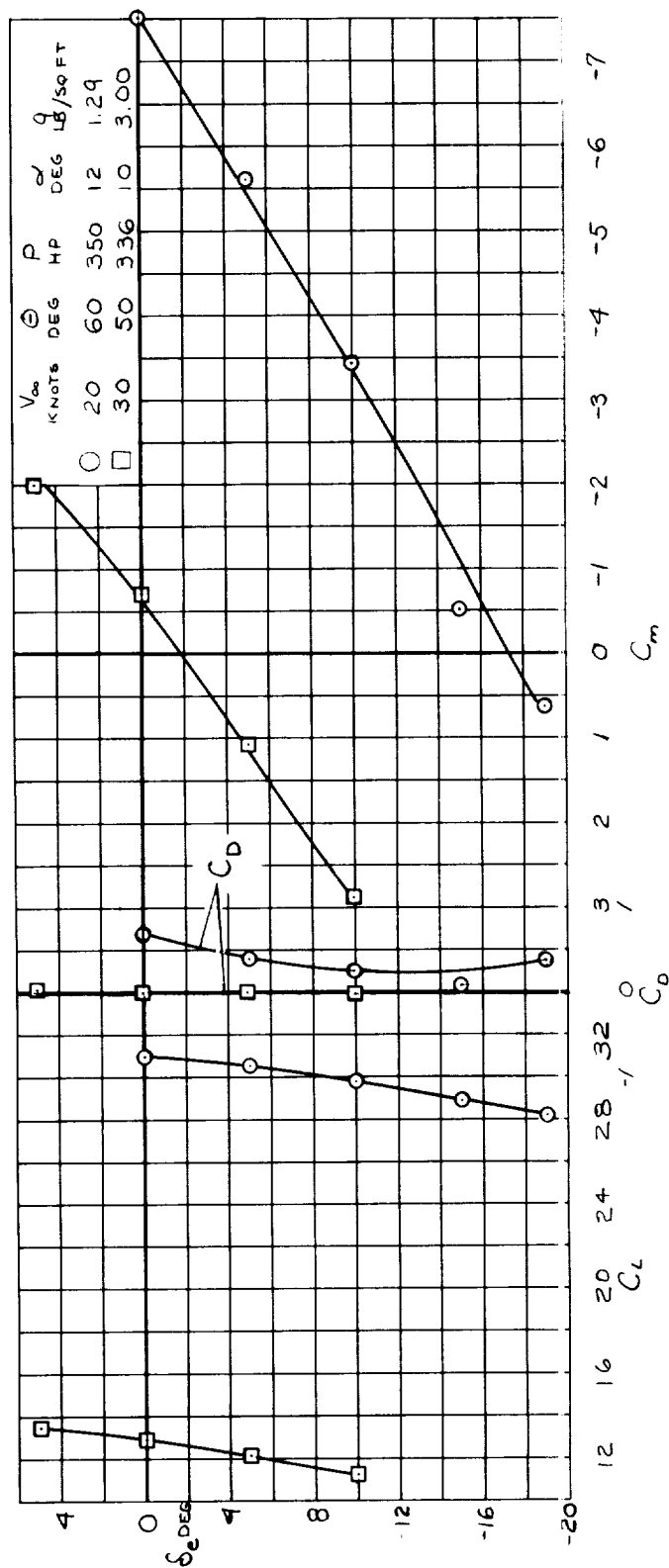
(e)  $V_\infty = 50$  knots;  $\theta_F = 31^\circ$ .

Figure 4.- Continued.



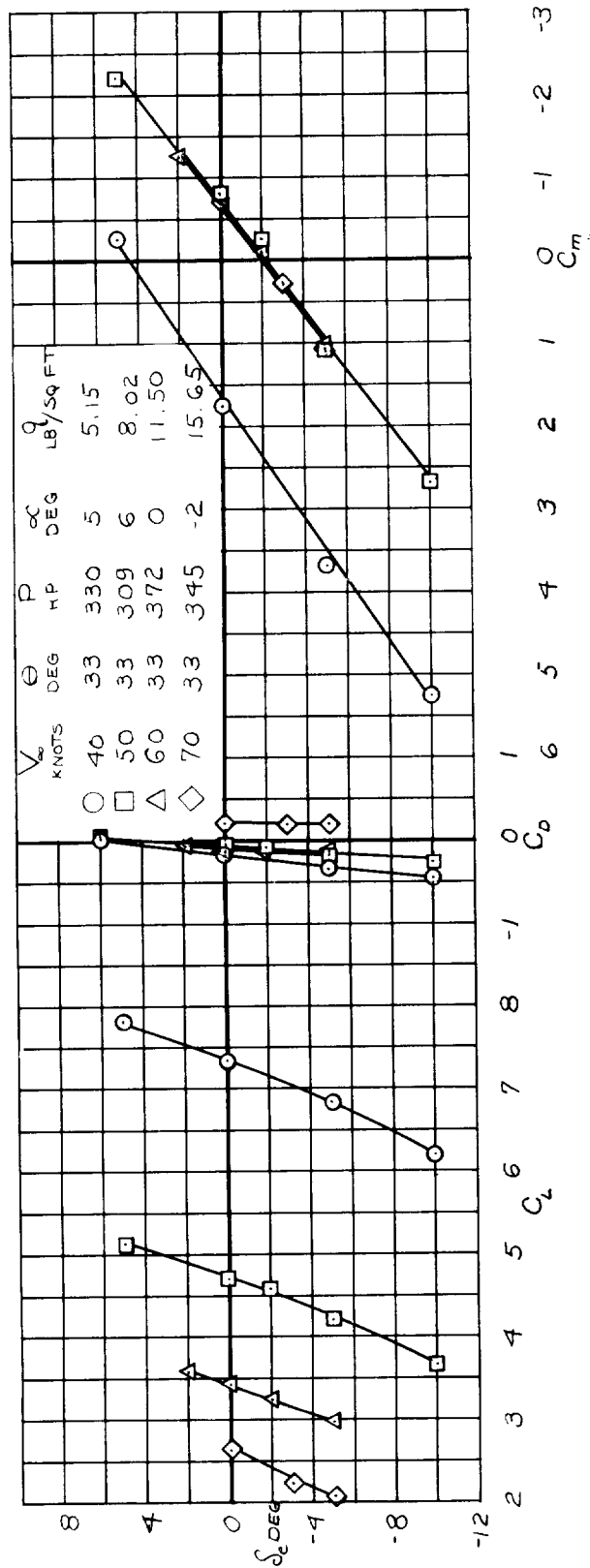
(f)  $V_\infty = 60$  and 70 knots;  $\theta_F = 31^\circ$ ;  $\theta = 33^\circ$ .

Figure 4.- Concluded.



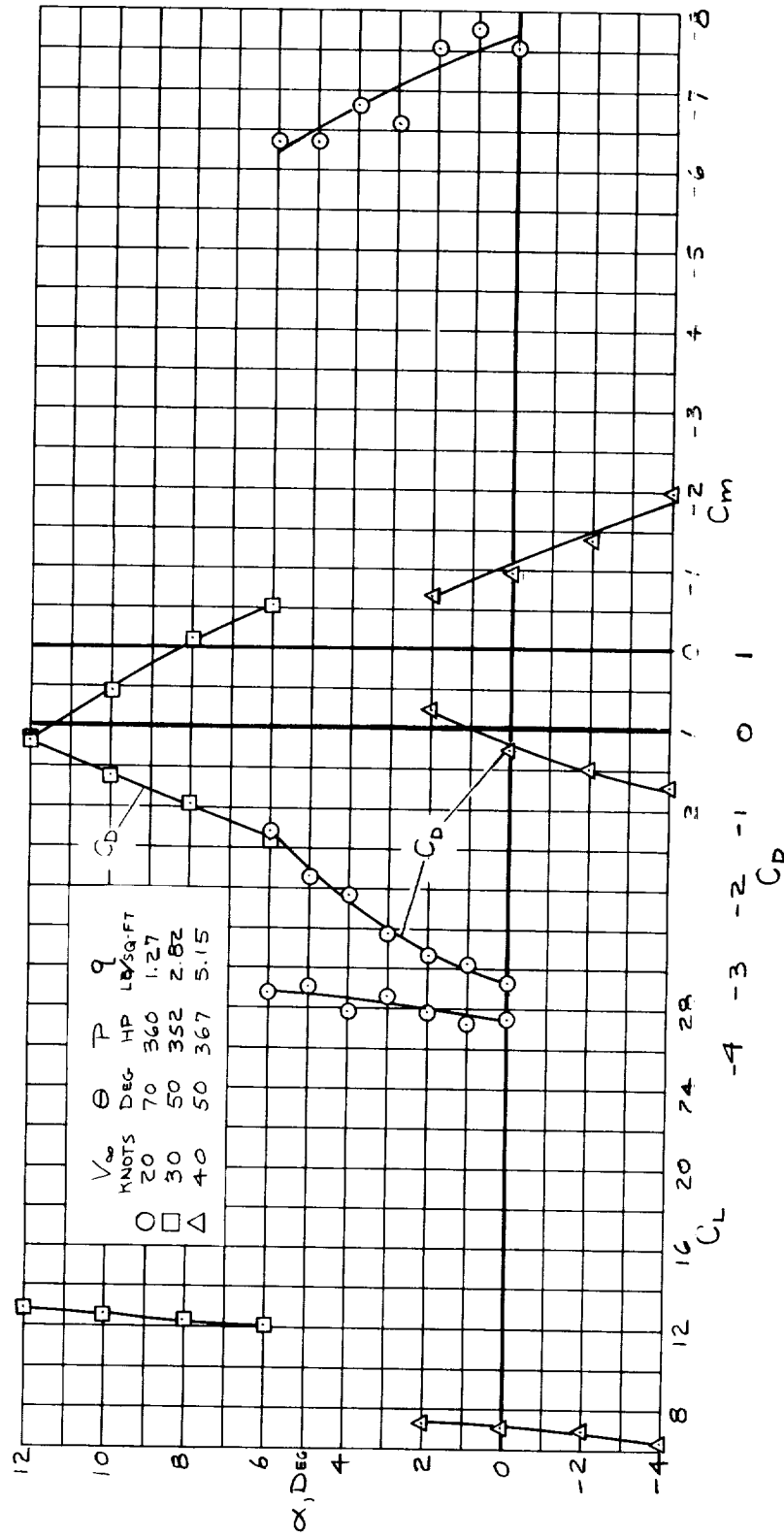
(a)  $V_\infty = 20$  and 30 knots;  $\theta_F = 66^\circ$ .

Figure 5.- Characteristics of the aircraft with the horizontal tail on; elevator deflection varying; fixed vane, F, out.



(b)  $V_\infty = 40, 50, 60,$  and  $70$  knots;  $\theta_F = 31^\circ$ .

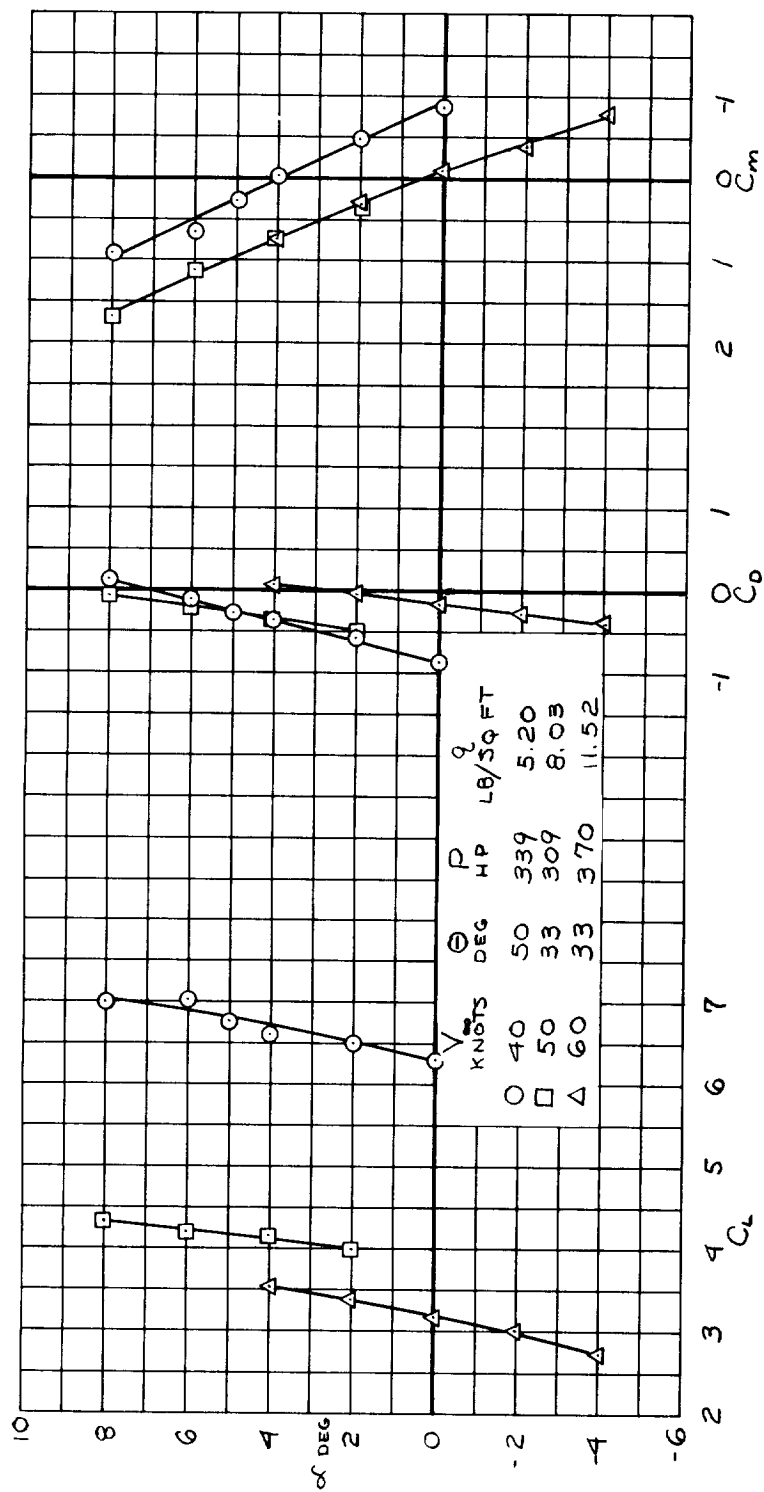
Figure 5.- Concluded.



(a) V<sub>∞</sub> = 20, 30, and 40 knots; θ<sub>F</sub> = 66°.

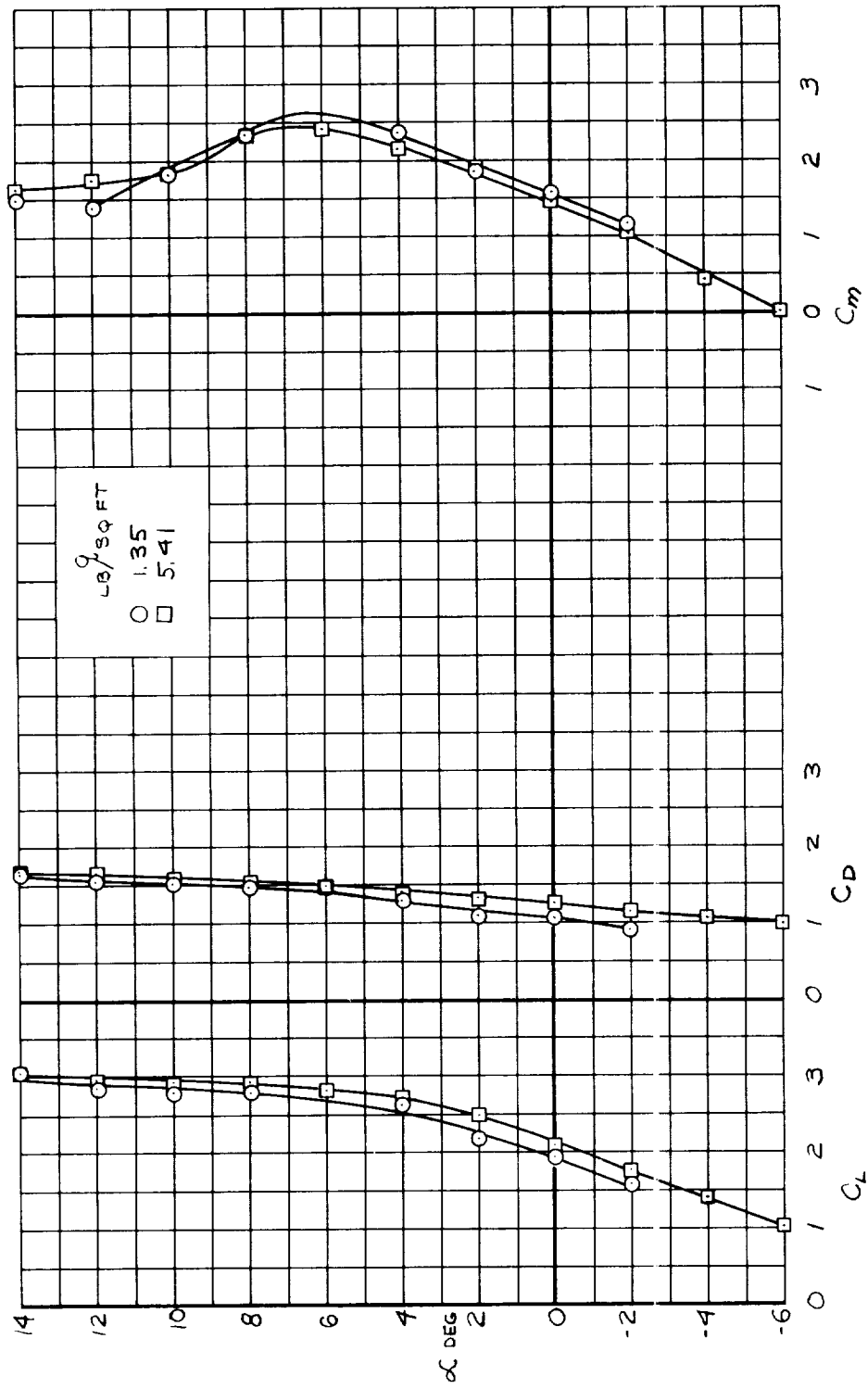
Figure 6.- Characteristics of the aircraft without horizontal tail; fixed vane, F, out.

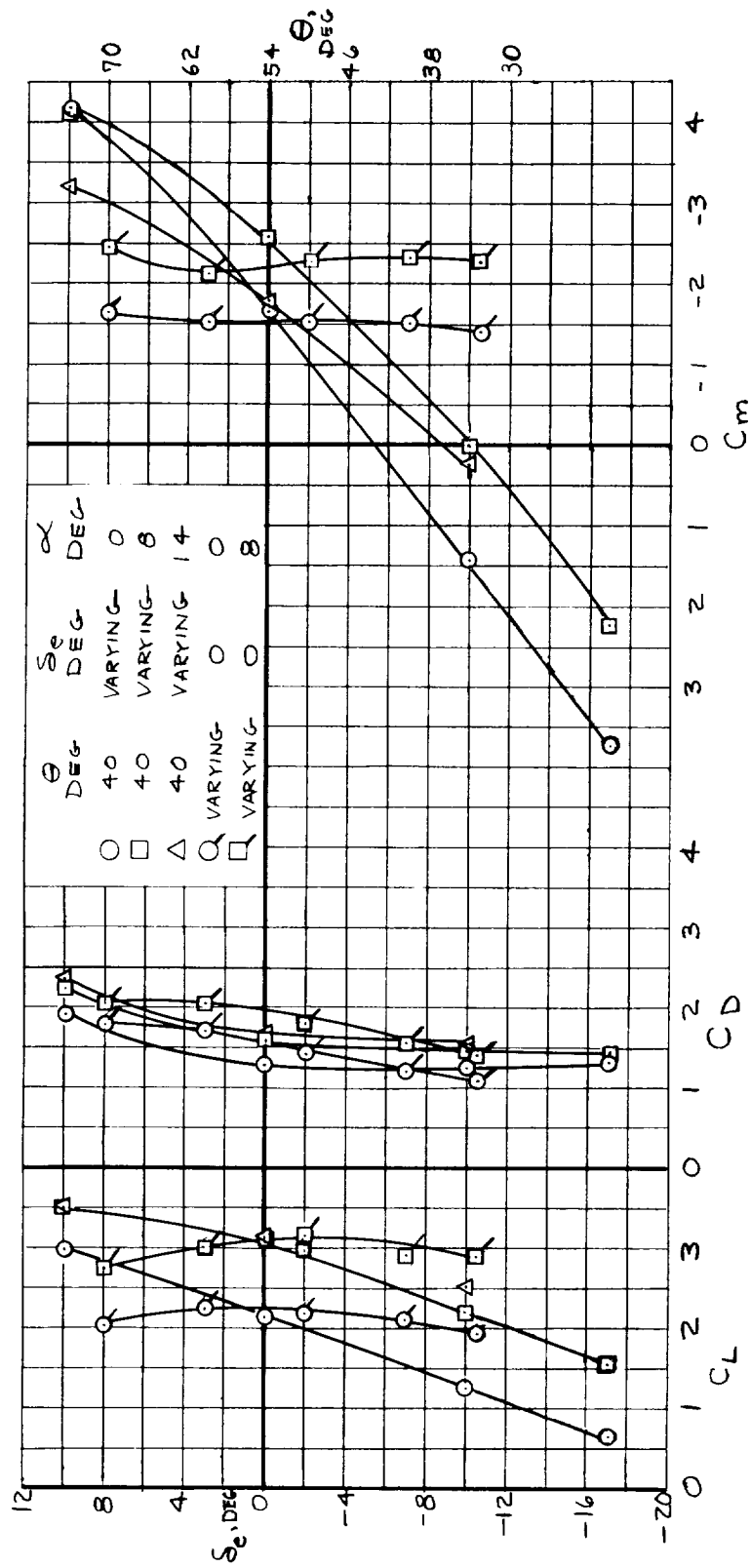




(b)  $V_\infty = 40, 50$ , and  $60$  knots;  $\theta_F = 31^\circ$ .

Figure 6.- Concluded.

(a)  $\alpha$  varying;  $\delta_e = 0$ .Figure 7.- Characteristics of the aircraft with power off;  $\theta_F = 31^\circ$ ;  $\theta = 40^\circ$  unless varying; propeller removed; fixed vane, F, out.



(b)  $\theta$  and  $\delta_e$  varying;  $q = 5.4 \text{ lb/sq ft}$ .

Figure 7.- Concluded.

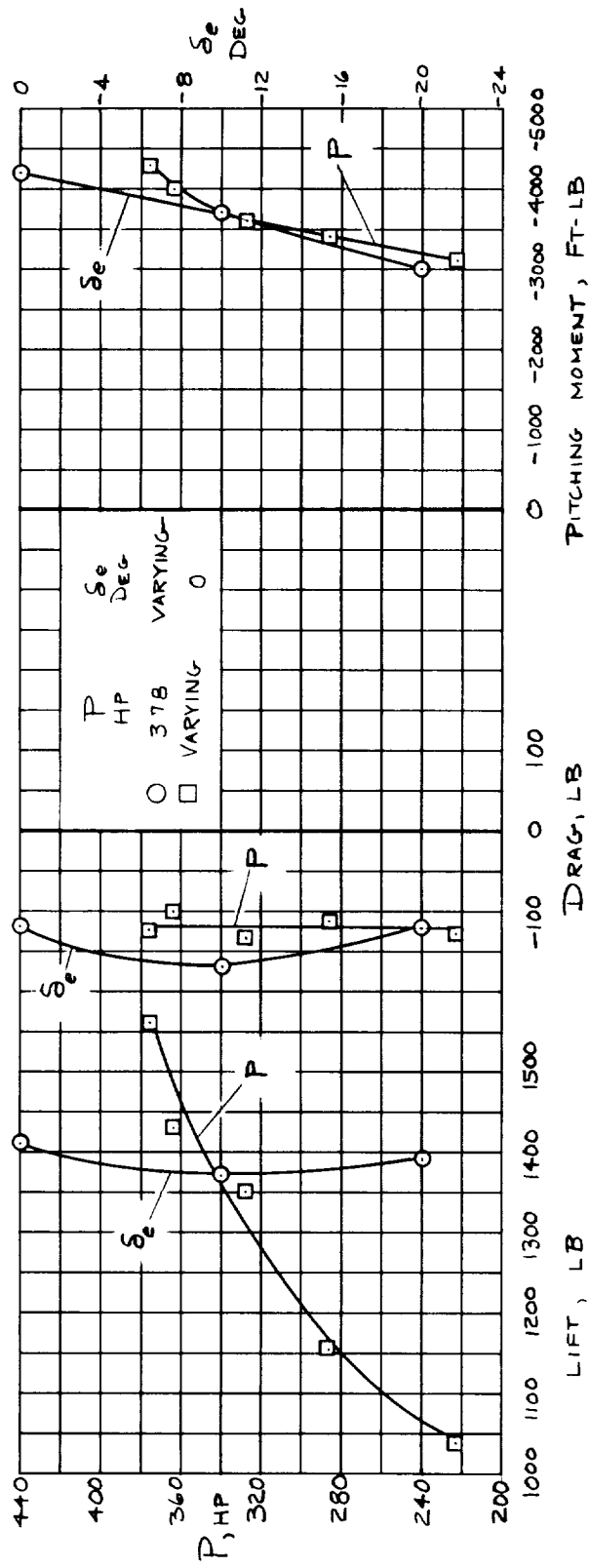
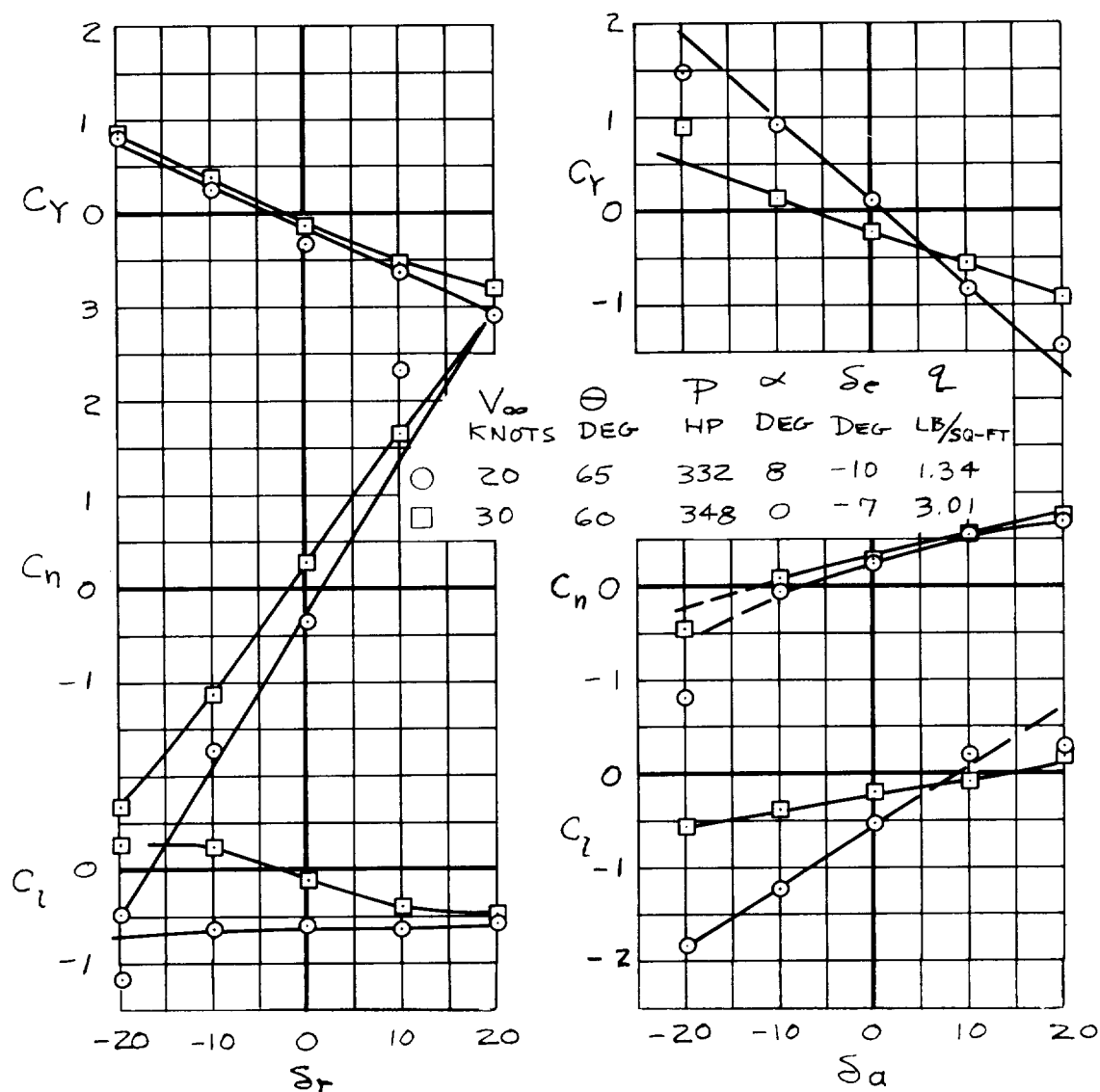


Figure 8.- Forces and pitching moment with  $V_\infty = 0$  at  $20^\circ$  angle of attack;  $\theta_F = 66^\circ$ ;  $\theta = 70^\circ$ ; fixed vane, F, in.



(a)  $\theta_F = 66^\circ$

Figure 9.- Effect of rudder and roll control deflection on the lateral characteristics.

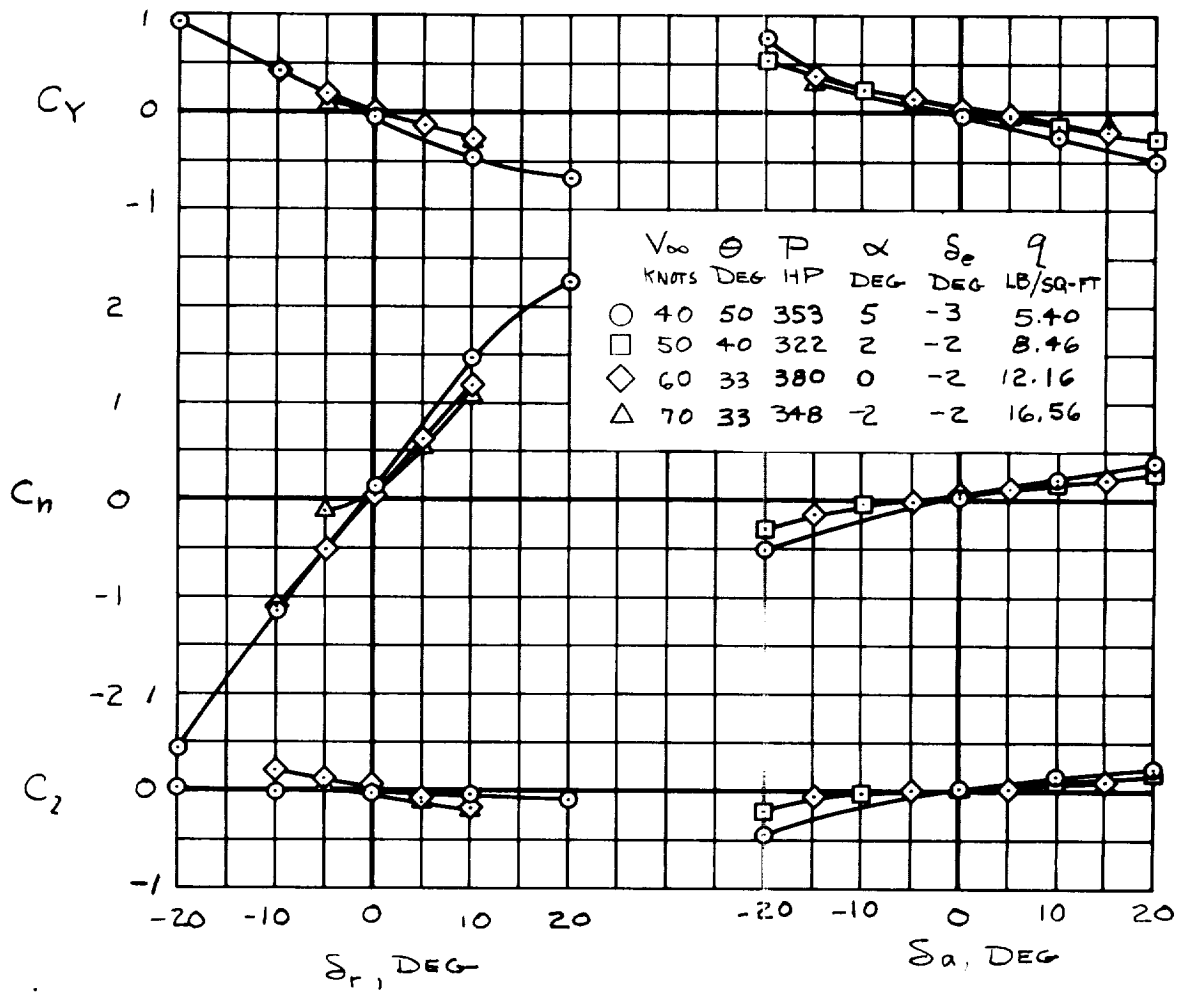
A  
4  
2  
0(b)  $\theta_F = 31^\circ$ 

Figure 9.- Concluder..

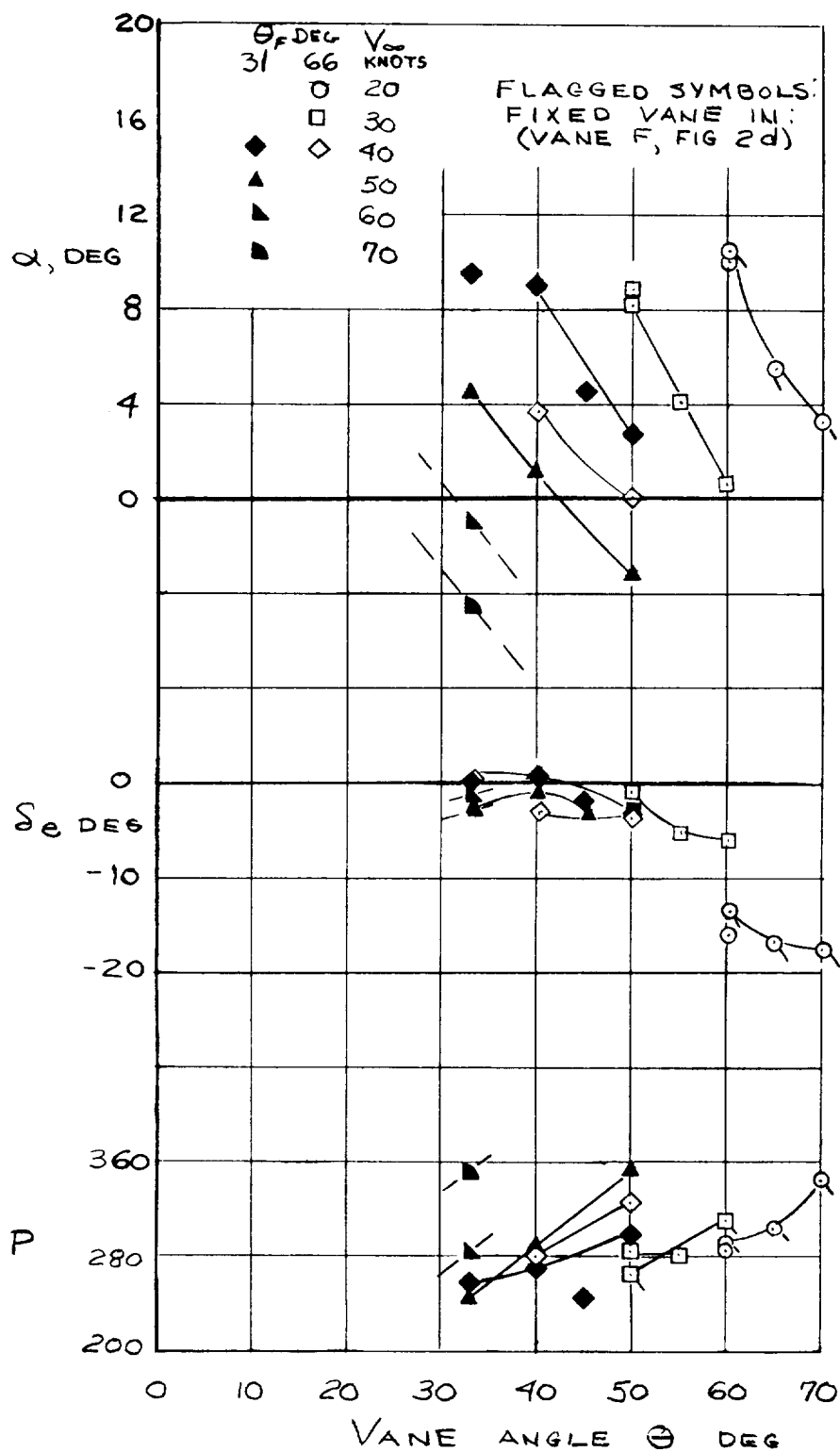
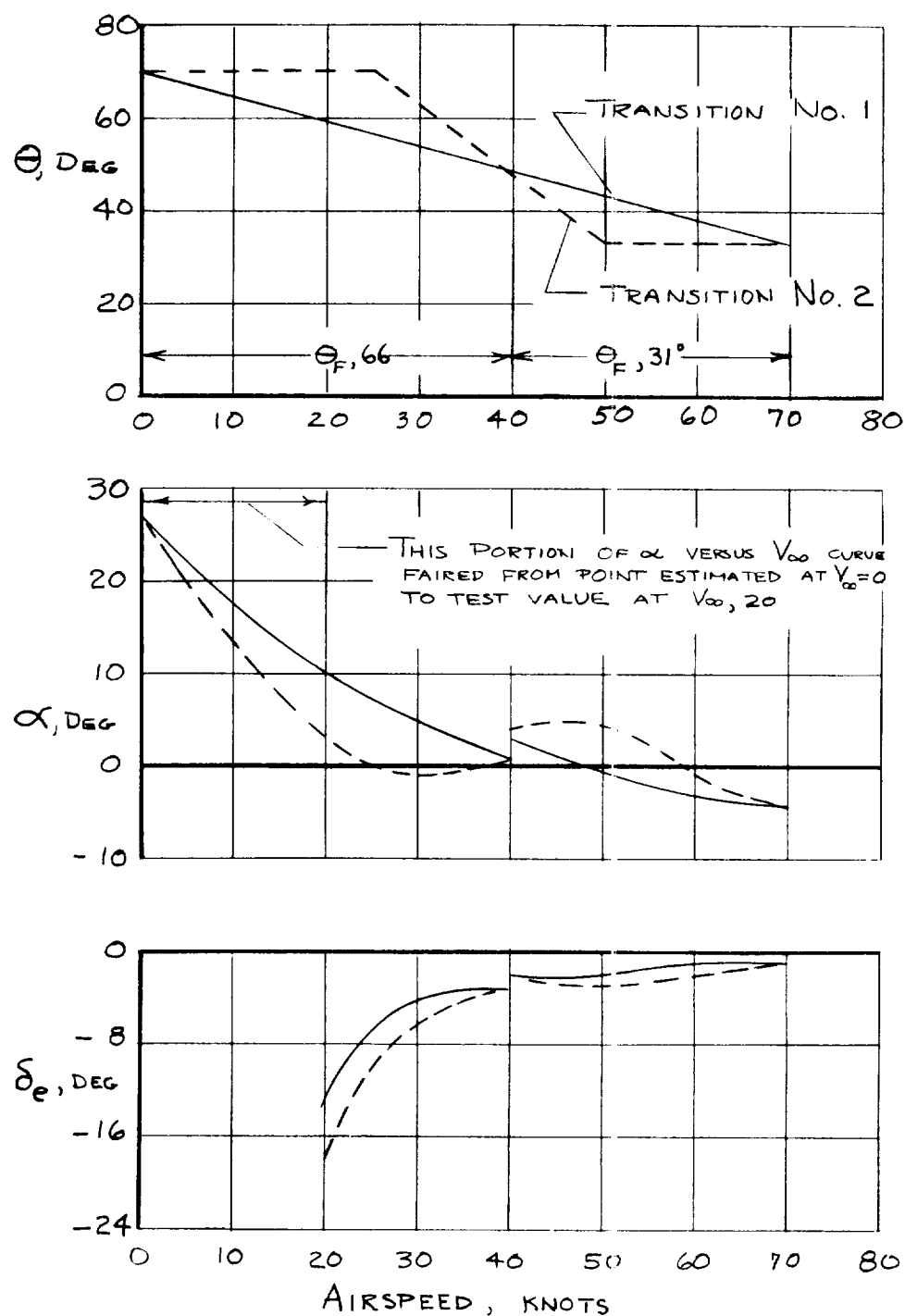


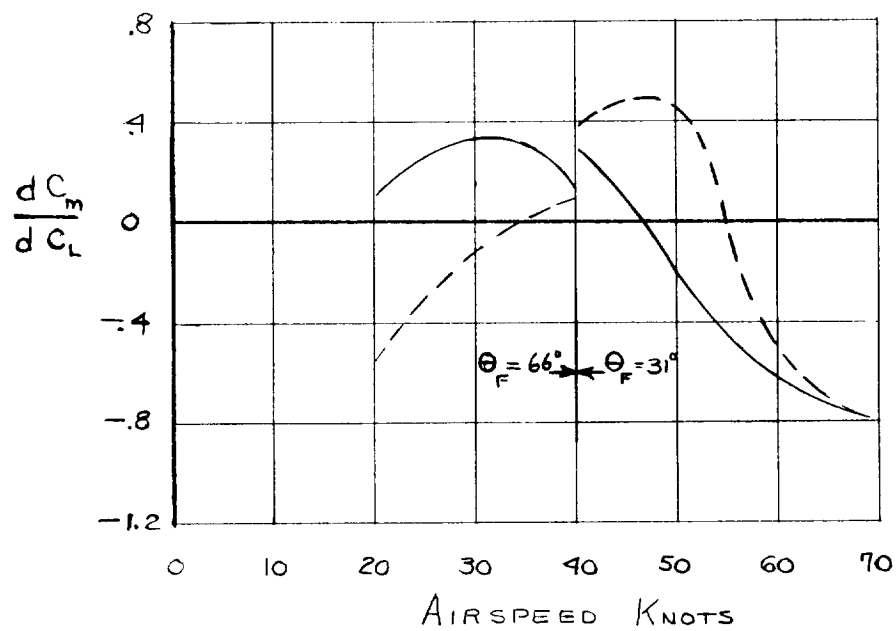
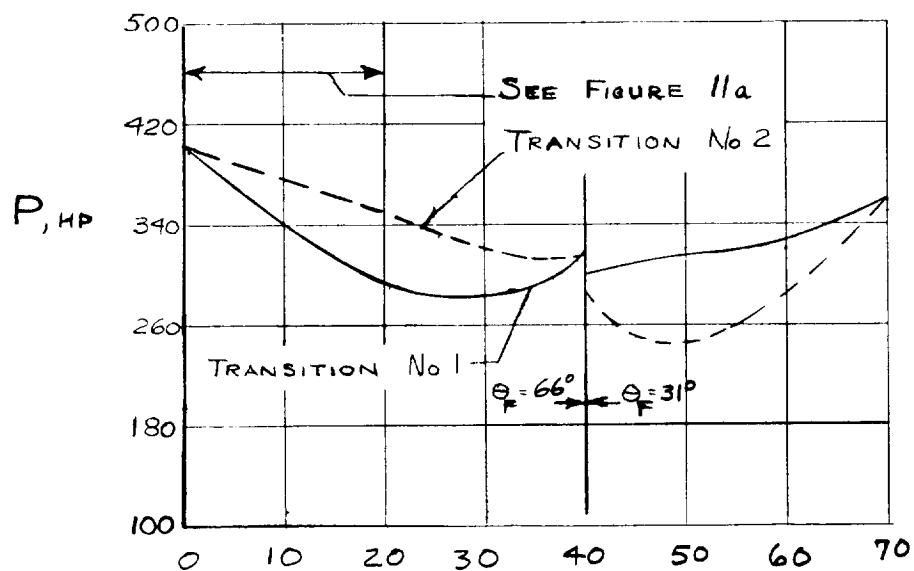
Figure 10.- Control and power settings required for trim at  $L=1500$  lb.



(a)  $\theta$ ,  $\alpha$ , and  $\delta_e$  versus  $V_\infty$ .

Figure 11.- Control and power settings for two trim level-flight variations of vane setting.





(b)  $dC_m/dC_L$  and  $P$  versus airspeed.

Figure 11.- Concluded.



<p><b>NASA TN D-326</b> National Aeronautics and Space Administration. LARGE-SCALE WIND-TUNNEL TESTS OF A WING-LESS VERTICAL TAKE-OFF AND LANDING AIR-CRAFT - PRELIMINARY RESULTS. David G. Koenig and James A. Brady. October 1960. 39p. OTS price, \$1.00. (NASA TECHNICAL NOTE D-326)</p> <p>Tests were made of an aircraft design based on a flying duct principle. Propellers enclosed in the duct provide propulsion at forward speeds where the duct provides most of the lift. Exit vanes in the duct deflect the duct flow downward to provide lift at or near zero forward speed. Force and moment data are presented for tests made at zero sideslip for velocities between 0 and 70 knots and exit vane angles between 33° and 70°.</p>	<p>I. Koenig, David G. II. Brady, James A. III. NASA TN D-326 (Initial NASA distribution: 1, Aerodynamics, aircraft; 3, Aircraft; 50, Stability and control.)</p>	<p><b>NASA TN D-326</b> National Aeronautics and Space Administration. LARGE-SCALE WIND-TUNNEL TESTS OF A WING-LESS VERTICAL TAKE-OFF AND LANDING AIR-CRAFT - PRELIMINARY RESULTS. David G. Koenig and James A. Brady. October 1960. 39p. OTS price, \$1.00. (NASA TECHNICAL NOTE D-326)</p> <p>Tests were made of an aircraft design based on a flying duct principle. Propellers enclosed in the duct provide propulsion at forward speeds where the duct provides most of the lift. Exit vanes in the duct deflect the duct flow downward to provide lift at or near zero forward speed. Force and moment data are presented for tests made at zero sideslip for velocities between 0 and 70 knots and exit vane angles between 33° and 70°.</p>	<p>I. Koenig, David G. II. Brady, James A. III. NASA TN D-326 (Initial NASA distribution: 1, Aerodynamics, aircraft; 3, Aircraft; 50, Stability and control.)</p>
<p><b>NASA TN D-326</b> National Aeronautics and Space Administration. LARGE-SCALE WIND-TUNNEL TESTS OF A WING-LESS VERTICAL TAKE-OFF AND LANDING AIR-CRAFT - PRELIMINARY RESULTS. David G. Koenig and James A. Brady. October 1960. 39p. OTS price, \$1.00. (NASA TECHNICAL NOTE D-326)</p> <p>Tests were made of an aircraft design based on a flying duct principle. Propellers enclosed in the duct provide propulsion at forward speeds where the duct provides most of the lift. Exit vanes in the duct deflect the duct flow downward to provide lift at or near zero forward speed. Force and moment data are presented for tests made at zero sideslip for velocities between 0 and 70 knots and exit vane angles between 33° and 70°.</p>	<p>I. Koenig, David G. II. Brady, James A. III. NASA TN D-326 (Initial NASA distribution: 1, Aerodynamics, aircraft; 3, Aircraft; 50, Stability and control.)</p>	<p><b>NASA TN D-326</b> National Aeronautics and Space Administration. LARGE-SCALE WIND-TUNNEL TESTS OF A WING-LESS VERTICAL TAKE-OFF AND LANDING AIR-CRAFT - PRELIMINARY RESULTS. David G. Koenig and James A. Brady. October 1960. 39p. OTS price, \$1.00. (NASA TECHNICAL NOTE D-326)</p> <p>Tests were made of an aircraft design based on a flying duct principle. Propellers enclosed in the duct provide propulsion at forward speeds where the duct provides most of the lift. Exit vanes in the duct deflect the duct flow downward to provide lift at or near zero forward speed. Force and moment data are presented for tests made at zero sideslip for velocities between 0 and 70 knots and exit vane angles between 33° and 70°.</p>	<p>I. Koenig, David G. II. Brady, James A. III. NASA TN D-326 (Initial NASA distribution: 1, Aerodynamics, aircraft; 3, Aircraft; 50, Stability and control.)</p>

\_\_\_\_\_

•

•

•

•

•

•